COMPARING THE EFFECTS OF A COMPREHENSIVE TYPICAL AMERICAN DIET OR MEDITERRANEAN DIET ON GUT MICROBIOME COMPOSITION

by

VIVIENNE LACY

Bachelor of Science, 2021
Texas Tech University
Lubbock, Texas

Submitted to the Graduate Faculty of the
College of Science and Engineering
Texas Christian University
in partial fulfillment of the requirements
for the degree of

Master of Science

May 2024

COMPARING THE EFFECTS OF A COMPREHENSIVE TYPICAL AMERICAN DIET OR MEDITERRANEAN DIET ON GUT MICROBIOME COMPOSITION

By

Vivienne Lacy

Thesis Approved:

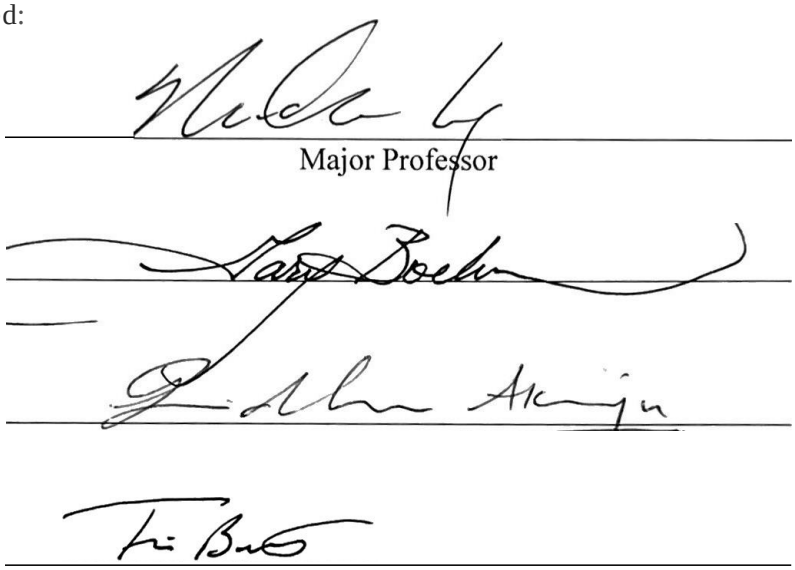

Major Professor

For the College of Science and Engineering

ACKNOWLEDGEMENTS

I am very thankful for the learning and growth opportunities that have I experienced during my time as a graduate student at Texas Christian University. I appreciate all of the faculty members that have helped me along the way. I would especially like to thank my graduate advisors, Dr. Mike Chumley and Dr. Gary Boehm, for providing guidance on this project and allowed me to focus on a new and exciting area for the lab. I would especially like to recognize Dr. Mike Chumley for the wisdom and optimism that has driven me to persevere this last semester. I would like to recognize the members of my graduate committee, Dr. Giridhar Akkaraju and Dr. Elisa Marroquin, for providing feedback on my thesis and working with me throughout my time at TCU. Additionally, I would like to thank Dr. Mike Allen and Dr. Yan Zhang, not only for their input and resources to complete this project, but also for their guidance and flexibility. Several of my fellow graduate students have helped me along the way and I would not have been able to graduate without their support and friendship. Most of all, I would like to reflect on my family pushing me to continue my education and supporting my decisions to complete my degree.

TABLE OF CONTENTS

LIST OF FIGURES

LIST OF TABLES

1. INTRODUCTION

It is currently estimated that 6.7 million Americans older than 65 years-of-age are living with Alzheimer's Disease (AD) (*Alzheimer's Association 2023 Annual Report*, 2023). This debilitating chronic disease is associated with cognitive decline, loss of independence, and changes in personality as well as the hallmark pathologies hyperphosphorylated tau tangles and amyloid beta (Ab) plaques (De-Paula et al., 2012). Tau is an intracellular microtubule-associated protein that when hyperphosphorylated, disassociates from the microtubules and aggregates into damaging neurofibrillary tangles (NFTs) leading to neuronal dysfunction and synaptic impairment (Drummond et al., 2020; Naseri et al., 2019). The other hallmark pathology, Ab plaques, are formed from cleavage of the amyloid precursor protein (APP) into $A\beta_{40}$ and $A\beta_{42}$ monomers which have the capacity to aggregate into plaques, thereby disrupting neuronal connections and causing cell death (Chen et al., 2017). While these pathologies contribute to the downstream effects associated with AD, the exact cause of AD remains mostly unknown. In the cases of early onset AD, the disease develops prior to the age of 65 and is due to known genetic mutations in APP and/or the enzymes that cleave APP. However, early onset AD is only responsible for 5% of cases diagnosed, leaving late onset AD to make up the majority of diagnoses (Mendez, 2019). Various environmental and lifestyle factors have been shown to increase the risk of developing late onset AD, including several modifiable factors such as chronic sleep loss, chronic stress, poor diet, and obesity (De-Paula et al., 2012).

In the United States, 41.9% of Americans are classified as having obesity and 9.2% as having severe obesity (Stierman, 2021). Several comorbidities are associated with obesity including type 2 diabetes, cardiovascular disease, and neurodegenerative diseases. While being classified as a BMI of 30 kg/m^2 or higher and an excess of fat accumulation (Purnell, 2023),

obesity is also associated with chronic inflammation, gut barrier dysfunction and dysbiosis, oxidative stress, and autophagy dysregulation–all of which are associated with an increased risk of developing AD. Multiple factors contribute to the development of obesity, with unhealthy dietary behavior being the most heavily contributing factor (Safaei et al., 2021).

The Western diet is the most common experimental diet model used in animal research to represent the dietary habits of Americans and is typically composed of excess saturated fats, simple carbohydrates, and low levels of fiber (Malesza et al., 2021). Chronic consumption of a Western diet results in negative peripheral effects such as increased white adipose tissue, dysbiosis of the gut microbiome, type 2 diabetes, non-alcoholic fatty liver disease (NAFLD), and chronic inflammation. Additionally, this diet is also associated with cognitive deficits, Ab aggregation, and an increased risk of developing neurodegenerative disorders including AD (Christ et al., 2019; Rakhra et al., 2020; Wieckowska-Gacek et al., 2021). While the Western diet is associated with several of the listed disease states, a Mediterranean diet (MD) has been shown to have protective properties against many of the same illnesses. The MD is commonly found in Italy and Greece and is associated with the consumption of poly-unsaturated fats, various sources of fiber, and diverse vegetables and fruits (Aridi et al., 2017). In human-based studies, strict adherence to a traditional MD is associated with a decreased risk of cognitive decline, decreased risk of developing type 2 diabetes, and a delay in the progression of AD (Abuznait et al., 2013; Andreu-Reinon et al., 2021; Stefaniak et al., 2022). In mouse models, various components of the diet such as olive oil, sulforaphane, and resveratrol, supplemented to the normal animal chow, has been shown to decrease inflammation, protect against cognitive decline, and decrease Ab in the brain (Abuznait et al., 2013; Borra et al., 2005).

While these versions of a Western diet and MD are commonly used as models in rodent research, neither experimental diet depicts what a typical American or typical person in the Mediterranean consume daily. Experimental Western diets are often exceedingly high in fat or sugar, often composed with up to as 60% kilocalories (kcal) from fat (Wieckowska-Gacek et al., 2021; Wu et al., 2023; Wu et al., 2021). This greatly contrasts the 30-35% kcal from fat that a typical American regularly consumes, thus limiting the translatability of these results. Most human research focusing on the MD looks at the percent adherence wherein it compares the characteristics of an individual's diet to a traditional Mediterranean diet, with a stricter adherence of an individual's diet associated with longevity benefits (Trichopoulou et al., 2015; Trichopoulou et al., 2014). Mediterranean diet studies in rodents typically only supplement regular rodent chow with one component of this complex diet, such as olive oil, to observe the physiological and protective effects, thereby limiting the comprehensiveness of the study (Abuznait et al., 2013; Haskey et al., 2022). To address these limitations in the literature, our lab, in association with Texas Christian University's Nutrition Department, designed two comprehensive diets to explore the effects of a typical American diet (TAD) and a Mediterranean diet (MD) based on the reported kcal percentages of macronutrients obtained from each region. Interestingly, typical Americans and those in the Mediterranean region consume diets that are similar in mean macronutrient levels, with 35% of their caloric intake from fat, 50% from carbohydrates, and 15% from protein. Therefore, the diets our lab created are similarly macronutrient-matched.

We previously conducted a long-term diet study utilizing our macronutrient-matched diets in which rodents were weaned onto and thereafter fed either the TAD or MD for 6-months. Peripheral and central inflammatory cytokines, Ab levels in the brain, and behavior and cognitive

measures were assessed at the end of the study. Proinflammatory cytokines TNF-α and IL-1β were measured by analyzing both the levels of the cytokine proteins in the serum and mRNA levels in the dorsal hippocampus. Analysis of the proinflammatory cytokines revealed an increased inflammatory profile in male and female mice consuming the TAD compared to mice consuming the MD. Spatial memory measured through the object location memory task (OLM) and anxiety-like behavior measured through the elevated zero paradigm indicated significant cognitive impairment of male TAD mice compared to male MD mice. This was supported by an increased level of soluble amyloid beta in the dorsal hippocampus of both male and female mice consuming the TAD. Additionally, mice fed the TAD had a significantly higher amount of fat in the liver, commonly indicative of NAFLD. While the results of this study were similar to previously published rodent studies using a high fat/sugar Western diet or supplements of a Mediterranean diet, we were the first to report on comprehensive diets more representative of the actual macronutrient composition that humans from their respective region would consume (Braden-Khule, 2024). Therefore, the translational aspect of this rodent TAD and MD merits further investigation.

The initial study comparing the TAD to the MD focused on the effects of these two diets in the lens of inflammation and AD pathologies. However, it has been well established that food composition has a significant impact on the gut microbiome and that gut microbiome dysbiosis caused by poor diet is associated with AD (Malesza et al., 2021; Pistell et al., 2010). In a previous study, we showed that mice consuming a synthetic amino acid formulated diet led to a significantly shifted gut microbiome after only one week (Mancilla et al., 2023). Because our TAD and MD experimental diets contain different food sources, the gut microbiome composition is expected to have varying characteristics While it is unknown whether differences in bacteria

abundance are the cause of disease development or a consequent result, understanding the microbiome composition is still relevant. The gut microbiome is primarily composed of bacterial species that colonize the intestinal tract and are responsible for harvesting energy, modulating the immune response, and producing key vitamins (Kesika et al., 2021). Energy harvesting occurs through the fermentation of non-digestible carbohydrates, leading to the production of short-chained fatty acids (SCFAs) including butyrate, propionate, and acetate. SCFAs increase the energy available to the host and act as local and system signaling molecules (Montenegro et al., 2023). Butyrate, propionate, and acetate regulate hepatic lipid and glucose homeostasis (Ott et al., 2018), with butyrate also regulating intestinal gluconeogenesis (Mtaweh et al., 2018; Sanchez-Delgado & Ravussin, 2020) and acetate suppressing adipocyte lipolysis and improving the insulin response (Primec et al., 2017). Further, butyrate maintains gut barrier integrity by increasing tight junction protein levels and serves as the primary energy source of colonocytes (Kesika et al., 2021). Propionate acts as a nutrient sensor which can reduce food intake and reduce cholesterol synthesis (Westerterp, 2017). Acetate and butyrate are primarily produced by bacteria within phylum Bacteroidetes, and butyrate produced by bacteria in the phylum Firmicutes (den Besten et al., 2013). The importance of SCFAs has been highlighted in metabolic health due to their role as signaling molecules that are responsible for the cross-talk between the microbiome and body.

A healthy gut microbiome is vital for the development and maturity of the immune system. In humans, the initial colonization of the gut microbiome occurs at birth, with the intestinal microbiome of the infant mirroring the bacteria found in the vaginal canal. The initial microbiome continues to change as the infant is exposed to its environment, with the microbiome beginning to stabilize and resemble a mature microbiome at 3 years of age (Mackie et al., 1999).

As the early life microbial composition may still be reflected in adult microbiomes, the early life period is an important time for immune education to occur which may lead to differing susceptibility to disease later in life. In early life, the human immune systems consist of immune cells that tend to develop tolerance following antigen exposure. This preference leads to the commensal bacteria that make up the microbiome to educate the immune system about what should and should not elicit a response (Spor et al., 2011). In germ-free mice, introducing commensal bacteria later in life restores some accrued deficits but still causes a different composition in the jejunum and colon. This suggests that the early-life window of colonization causes irreversible consequences that may lead to a differentially developed immune system in an adults (El Aidy et al., 2013).

Mucosal immunity plays an important role in immunomodulation wherein the immune system is tolerant of the bacteria comprising the gut microbiome, but is sensitive to overgrowth and translocation of bacteria into the rest of the body. Immune deficiencies are observed in germ-free mice, partially due to the lack of molecular effectors produced by intestinal bacteria (Hevia et al., 2015). For example, lipopolysaccharide (LPS), the outer membrane component of gram-negative bacteria, from non-pathogenic bacteria helps train the immune system early in life, and communicates microbiome health to the immune (Kesika et al., 2021). Bacterial overgrowth can lead to dysbiosis and infection, such as accumulation of *Helicobacter pylori,* causing peptic ulcers (Araujo et al., 2022). Translocation of bacteria or their toxins into systemic circulation can lead to complications including eliciting an immune response or causing infection. Chronic inflammation weakens intestinal permeability by debilitating the tight junctions between enterocytes, further elevating bacterial translocation and systemic inflammation, thus creating a vicious circle (El Aidy et al., 2013). Inflammation can also be used by several pathogens to

decrease the viability of the gut microbiome, allowing the pathogens to maximize their infective potential and establish themselves in the gut microbiome. Many pathogens from the phylum Proteobacteria use inflammation to aid in their colonization, such as *Salmonella enterica serovar Typhimurium* (Lupp et al., 2007; Stecher et al., 2007). Conversely, a diverse microbiome composition limits pathogenic colonization by diminishing nutrient and space (niches) availability and by increasing the production of anti-microbial peptides (Kesika et al., 2021). Maintaining immune tolerance and sensitivity to pathogenic bacteria relies on a microbiome in *eubiosis*.

A healthy gut microbiome is one that is rich in phyla Firmicutes, Bacteroidetes, Actinobacteria (Garcia-Montero et al., 2021), Verrucomicrobiota, and Proteobacteria (Kesika et al., 2021). Nonetheless, the specific bacterial species associated with a healthy gut microbiome are still to be determined. However, having increased microbial diversity has been consistently associated with a healthy gut microbiome. Strict adherence to a MD has been correlated with an increase in favorable bacterial species, limited growth of pathogenic bacteria including LPS-producing Enterobacteria, and an increase in beneficial bioactive metabolites (Garcia-Montero et al., 2021). Components of the MD, such as plant polyphenols and dietary fiber, have been associated with increased microbial diversity and SCFA fermentation (Garcia-Montero et al., 2021). Overall health is influenced, however, not only by the presence of specific bacteria, but also by the levels and ratios of cohabitating bacteria, viruses, and archaea.

The specific composition of a microbiome in dysbiosis is also largely undefined, however gut microbial dysbiosis is generally associated with decreased microbial diversity as well as an increase in the abundance of pathogenic species. Consumption of the Western diet is associated with gut microbiome dysbiosis and the development of several diseases states previously

mentioned. A high-fat Western diet is associated with a significant decrease in various SCFAs (Agus et al., 2016), an increase in intestinal permeability, and an increased pro-inflammatory immune response (Bruce-Keller et al., 2015). Significantly reduced diversity and differing community structures causing a decrease of gut barrier bacteria have also been linked to consumption of a Western diet (Statovci et al., 2017). Chronic systemic inflammation from dysbiosis can over activate brain microglia and weaken blood brain barrier permeability, leading to neuroinflammation and neuronal damage. Long-term gut microbiome dysbiosis has been associated with chronic disease states, ranging from inflammatory bowel disease (IBD) to an increased risk of developing AD due to the bidirectional signaling within the gut-brain axis (Kesika et al., 2021). Communication between the gut and the brain occurs through the production of gut-derived neurotransmitters and modulators or by direct bacteria translocation (Pluta et al., 2020).

While there is an established link between AD pathologies and gut microbiome dysbiosis, the current experimental literature has the major limitation of using Western diets that are excessively high in fat and sugar. Therefore, the purpose of this study was to explore the effects of long-term consumption of a realistic TAD and MD on the composition of the gut microbiome. Additionally, the transgenerational effects of the two diets were explored to examine the possible effects of perinatal diet on the gut microbiome during development and early life. The offspring mice would be on the experimental diet during the key early window in which the immune system is malleable, then at post-natal day 21 shifted towards the standard rodent diet. We expect the initial offspring microbiome composition to resemble that of their mothers and thus continue showing compositional differences depending on their mother's experimental diet. Furthermore, we hypothesize that these early differences in the offspring's microbial composition may lead to

differential immune training and tolerances. After weaning onto standard diet, we expect the gut microbiomes of offspring birthed from either experimental group to become the same except for a few, probably undetectable, differentially abundant bacteria due to the fingerprint that early-life gut microbiome composition has on adults.

2. METHODOLOGY

2.1 Study Design and Animal Use

Parental Generation (G1)

31 male and 23 female C57BL6/J mice bred in Texas Christian University's vivarium were utilized in this study. A baseline fecal sample was collected from the animals on postnatal day 21 (PND 21) after which each mouse was randomly assigned to one of two long-term experimental diet conditions; 1) a typical American diet (TAD; D21112903) or 2) a Mediterranean diet (MD; D21112902) both formulated at Research Diets (New Brunswick, NJ). Animals were maintained on these diets for 6 months and fecal samples were collected after 1 month on the diet and after 6 months on the diet (Figure 1). The experimental diets were formulated by Texas Christian University's Nutrition Department and the Neurobiology of Aging Laboratory (see Table 1 for diet composition). This initial experimental group of 54 animals comprised the parental generation (G1) of the study.

Table 1. Dietary Components and Macronutrient Percentages. Macronutrient percentages and key dietary components of the Mediterranean diet (MD) and typical American diet (TAD). Both diets' macronutrient percentages were 50% from carbohydrates, 35% from fat, and 15% from protein. The dietary sources listed are representative for the respective region.

Key Dietary Components	Mediterranean Diet	Typical American Diet	Macronutrient Percentage
Carbohydrates	Brown rice & wheat starch	Corn starch	50%
Fats	Olive oil, fish oil, & flaxseed oil	Beef Fat (Bunge), Safflower Oil, Butter (Anhydrous)	35%
Protein	Egg whites, soy, & fish protein	Casein (from milk fat)	15%

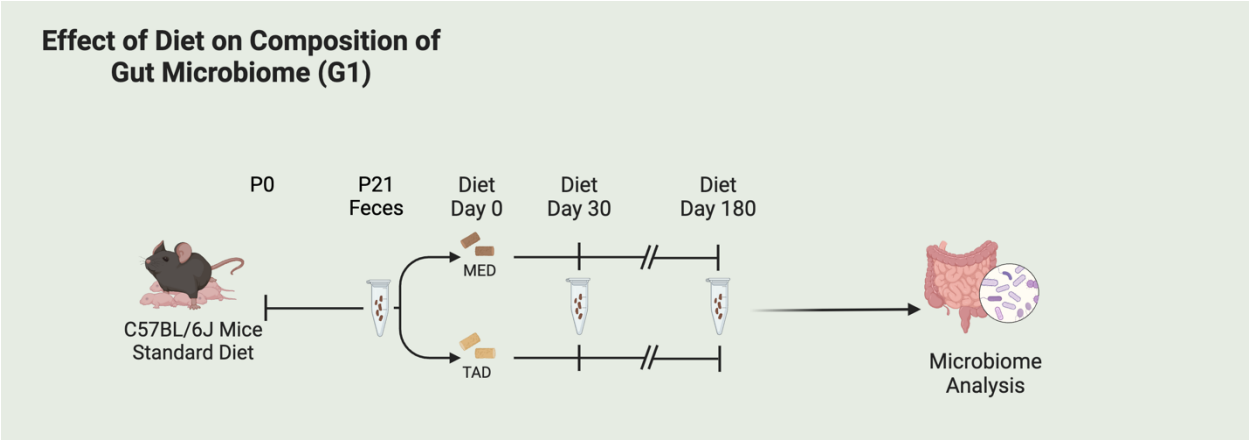

Figure 1. Graphical experimental timeline of parental (G1) generation mice. Baseline fecal pellets were collected at PND 21 with the animals later divided and weaned into either the experimental MD or the TAD. Additional fecal collection timepoints included 1 month (2 months of age) and 6 months post-intervention (7 months of age). Collected fecal pellets were used for downstream analysis of the gut microbiome composition.

Offspring Generation (F1)

After sampling the final fecal collection, a small subset of males and females in each diet group were paired to maintain their respective diet condition and allowed to breed to produce the first generation (F1) to explore the transgenerational effects of diet (Figure 1). The parental subset animals (1 male and 1 female per cage) remained on their respective experimental diet throughout breeding until offspring were weaned. F1 offspring (*n*'s = 22) baseline fecal samples were collected on PND 21 prior to being weaned onto standard rodent chow (Lab Diet Prolab RMH 1800). F1 generation mice were housed according to parental diet conditions (MED born offspring housed with MED born offspring, TAD born offspring housed with TAD born offspring) and remained on standard rodent chow until their final fecal collection at 2-3 months on diet.

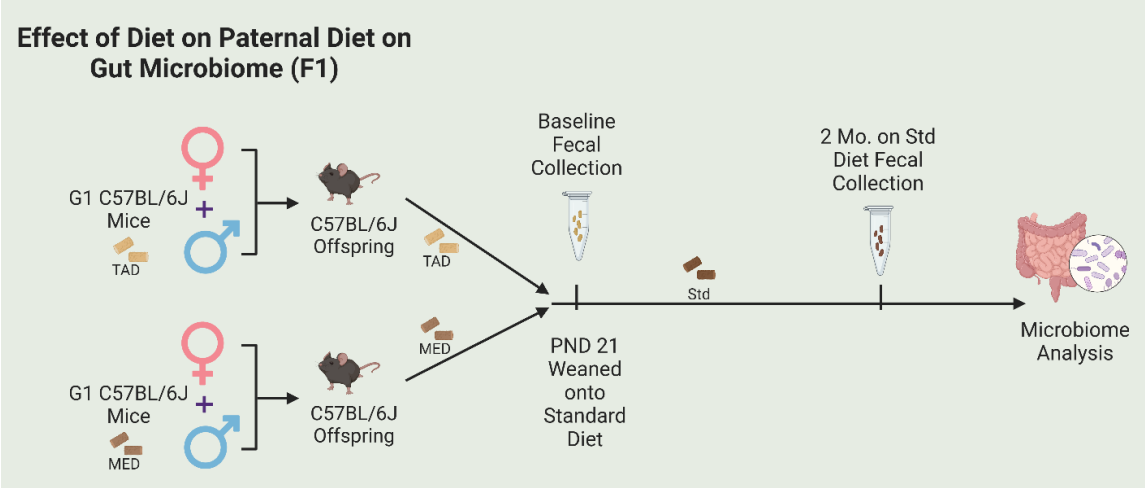

Figure 2. Graphical experimental timeline of offspring (F1) generation mice. G1 mice were bred within diet condition, with the offspring exposed to experimental diet throughout gestation and early life. Baseline samples were collected from offspring on PND 21 prior to weaning onto standard rodent chow. Subsequent sampling occurred at 2-3 months on standard diet (3-4 months of age). Collected fecal pellets were used for downstream analysis of the gut microbiome composition.

Subject Parameters

All non-breeding animals were group housed (3-4 animals per cage) in polycarbonate cages with pelleted, paper-chip bedding and compressed cotton square nestlets (LabSupply, Fort Worth, TX) under a 12-hour light/dark schedule within diet condition and provided food and water *ad libitum*. All procedures and handling complied with the Guide for the Care and Use of Laboratory Animals (National Research Council, 2011) and were approved by TCU's Institutional Animal Care and Use Committee (IACUC Protocol # 2021-14).

2.2 Sample Processing

Sample Collection

Animals were temporarily individually housed in 12.5cm X 15cm X 25cm empty polycarbonate cages for fecal collection. Once 2-3 pellets were collected with tweezers, fecal samples were stored in sterile microcentrifuge tubes at -80℃ for further analysis and animals were returned to their original group housing. Baseline samples were collected from every animal prior to weaning. G1 fecal samples were collected at baseline, 1 month on diet (2 months of age), and 6 months on diet (7 months of age). F1 samples were collected at baseline and 2-3 months on diet (3-4 months of age).

Nucleic Acid Isolation

Nucleic acid isolation was performed using the MagMAX Microbiome Ultra Nucleic Acid Isolation Kit for fecal samples (ThermoFisher Scientific, Waltham, MA). Isolation was performed according to the MagMAX protocol, with the addition of 40uL proteinase K followed by a 30-minute incubation period at 56C during the sample lysis step for further extraction. Due to limited sample amount for baseline timepoints, elution volume was reduced to 100uL and a maximum volume of fecal sample of 50mg was used. Samples were run on the ThermoScientific KingFisher Flex (Waltham, MA) with the recommended protocol "MagMAX_Microbiome_Stool_Flex" (Appendix A) modified to account for 100uL of elution buffer. Isolated nucleic acid was measured using a Nanodrop 2000 Spectrophotometer (ThermoFisher Scientific).

Amplicon PCR and Gel Electrophoresis

Amplicon polymerase chain reaction (PCR) was performed to amplify the template region of interest. Amplicon PCR was performed on all samples in duplicate with a positive control of 15ng/mL *E. coli* genomic DNA and negative control of sterile molecular grade water. PCR Master Mix was comprised of Invitrogen 10X AccuPrime PCR Buffer II, Invitrogen 50mM

$MgSO_4$ (ThermoFisher Scientific), Illumina forward and reverse V4 primers (Illumina, San Diego, CA), 1.0mg/mL BSA, and 4mM AccuPrime TaqDN (ThermoFisher Scientific). DNA amplification was performed using the following protocol: denatured at 94C for 2:00min; 24 x (94C for 0:30 sec, 55C for 0:40 sec, 68C for 0:40 sec), and final extension at 68C for 5:00 min. Gel electrophoresis was performed on all PCR samples to confirm the presence of nucleic acid prior to proceeding to the next steps.

PCR Clean-Up and Index PCR

PCR clean-up was performed to free the samples from primers and primer dimer species. 32uL of AMPureXP beads (Beckman Coulter, Pasadena, CA) were added to each well of the Amplicon PCR plate and shaken for 2 minutes at 1800rpm. After a 5-minute room-temperature incubation period, the plate was placed on a magnetic stand until the supernatant cleared. With the PCR plate still on the magnetic stand, all supernatant was discarded and the remaining magnetic beads were washed twice with 80% ethanol for 30sec. The second ethanol wash was removed and the beads were air-dried for 10min while still on the magnetic stand. After incubation, the Amplicon PCR plate was removed from the stand and 52.5 uL of 10 mM Tris pH 8.5 was added to each well. The plate was incubated at room temperature for 2 minutes, placed on the magnetic stand until the supernatant cleared, then the supernatant was transferred to a new 96-well PCR plate. Index PCR was performed using the NexteraXT index kit V2 (Illumina) to attach dual indices and the Illumina sequencing adapters (Illumina) using a modified PCR thermal cycling program: denatured at 94C for 3:00min; 8x (95C for 0:30 sec, 55C for 0:30 sec, 68C for 0:30 sec), and final extension at 68C for 5 min. PCR cleanup was then performed using the same protocol previously listed. The DNA concentration in nM was calculated in order to dilute the concentrated final library to 4nM using 10mM Tris pH 8.5. The library was pooled by

adding 5uL of diluted DNA from each library and mixing. Specifically, the library pooling consisted of 30mL of working solution (1:200 of dsDNA HS Reagent in Qubit dsDNA HS buffer with 1uL of dye added) (ThermoFisher Scientific).

Library Denaturing and MiSeq Sample Loading

The final pooled DNA library consisting of all samples that are individually labeled with a unique barcode sequence was denatured in preparation for sample loading where cluster generation and sequencing would occur. The final 4mM pooled libraries were denatured with 0.2 N NaOH for 5 minutes. A control of 4pM PhiX (Illumina) was used throughout the library denaturing and sample loading process to serve as an internal control during the run. After the pooled library and PhiX control were denatured with 0.2 N NaOH, 10uL of the denatured contents were added to 990uL of pre-chilled HT1 (Illumina). The denatured sample DNA and PhiX control was diluted to a final concentration of 20pM. 30uL of denatured and diluted PhiX control and 570uL of denatured and diluted amplicon library were combined in a microcentrifuge tube prior to loading it onto the MiSeq v4 reagent cartridge. After preparation, the MiSeq reagent cartridge was loaded on the MiSeq flow cell (Illumina).

2.3 Statistical Analysis

FASTQ files generated by the Illumina MiSeq instrument were processed for microbiome analysis. The QIIME2 workflow (Bolyen et al., 2019) was followed in Miniconda3 throughout to process data, analyze data, and create visuals (see Appendix C for code used to generate all visuals). Raw sequences stored as FASTQ files were imported and underwent sequence quality control using the DADA2 pipeline (Callahan et al., 2016) to trim and truncate sequences based on quality scores from the demultiplexed data. Within the DADA2 pipeline, sequences were filtered, merged, and clustered. A feature table was generated using the mafft program to

generate a rooted tree for downstream phylogenetic diversity analysis. Taxonomic analysis was performed using the pre-trained Naïve Bayes classifier and the q2-feature-classifier plugin (Bokulich et al., 2018). Taxa bar plots were generated to view the taxonomic composition according to taxonomic levels of classification. Alpha and beta diversity analysis was generated using the q2-diversity plugin. Alpha group significance between categorical metadata columns was generated using Shannon diversity index and Evenness. Beta diversity was analyzed using PCoA plots using Emperor to generate weighted and Bray-Curtis Emperor plots. Beta group significance between categorical metadata columns was generated using a PERMANOVA. Differential abundance testing with ANCOM was used to identify features that are differentially present across sample groups, and data was filtered according to experimental group. Results from the differential abundance testing were filtered according to the specific taxonomic levels present.

3. RESULTS

3.1 Initial Microbial Analysis

To ensure no confounding variables were a part of the downstream analysis, sex and baseline differences were initially examined through comparing beta diversity metrics. Beta diversity provides information on the differences in microbial composition between different experimental communities and how they vary by taking into consideration the presence or absence of taxa and their relative abundances. Differences in community composition was measured using principal coordinate analysis (PCoA) as it relies on distance rather than variations for plotting and maximizes linear correlation. Typically, larger eigen values (the percentages over the respective axes), such as one whose axes add to over 50%, are considered

successful as they capture a significant percent of data variation. The PCoA plots were generated using Weighted UniFrac metrics, which gauge community dissimilarity while accounting for phylogenetic relationships. This approach detects distinctions stemming from variations in relative abundances rather than taxonomic presence. For beta diversity statistical results, a PERMANOVA was used as it tests if the distances between samples within one group are more similar to each other than samples from a different group. At all sampling timepoints throughout the intervention, there is complete overlap between samples according to sex, indicating there is no difference in gut microbiome community composition due to sex, as supported by a PERMANOVA (n = 70, permutations = 999, pseudo-F = 0.195, $p = 0.952$) thus we compressed samples across sexes for subsequent analyses between diets (Figure 3).

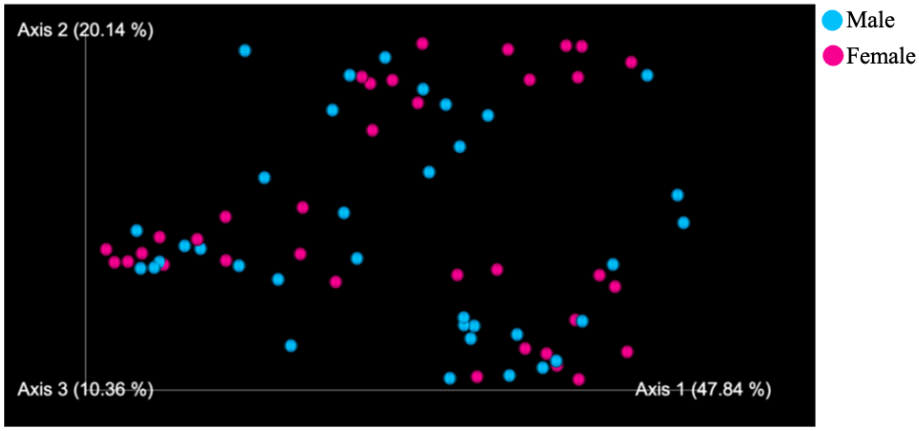

Figure 3. PCoA of Weighted UniFrac distances according to sex in G1. A principal coordinate analysis (PCoA) plot of weighted UniFrac distances revealed overlap according to sex, with individual samples represented by one dot. As no differences in overlap was observed, samples will be compressed across sexes for subsequent data analysis.

Baseline metrics were also compared using alpha and beta diversity to ensure no initial differences between experimental conditions. Alpha diversity is important to understand the diversity of microbial species within a specific experimental condition, such as diet. Two different metrics were used throughout the study to assess alpha diversity. Firstly, estimated richness, or the number of different species present, was measured number of operational taxonomic units (OTUs). Secondly, evenness, or the distribution of abundance between species, was calculated using Simpson's evenness. Prior to weaning when all experimental groupings were consuming standard rodent chow (0 MOD), there was no significant difference in mean Shannon diversity ($H = 0.011$, $p = 0.918$), Simpson's evenness ($H = 0.900$, $p = 0.343$), or observed OTUs ($H = 2.372$, $p = 0.123$) according to diet condition. Analysis of a PCoA plot of weighted UniFrac distances according to month on diet (MOD) revealed significant overlap within the 0 MOD timepoint for either experimental diet group. The baseline group will not be further explored as there was an overlap between both experimental groups at 0 MOD (PERMANOVA with 26 samples and 999 permutations performed, calculated pseudo-F statistic of 0.811 and a *p*-value of 0.453).

No overlap between 0 MOD and 6 months on diet (6 MOD) indicated a dramatic shift of community composition of the gut microbiome across timepoints due to the implementation of the experimental diet (Figure 4). PERMANOVA determined that the deviance based on MOD (0 MOD vs 6 MOD) was significant ($n = 42$, permutations = 999, pseudo-$F = 11.666$, $p = 0.001$). Experimental timepoints 1 month on diet (1 MOD) and 6 MOD were analyzed to explore the time it would take to fully shift the gut microbiome to a stable community. Beta diversity showed an overlap between 1 and 6 MOD, indicating no differences in microbial community

composition, therefore, the 6 MOD timepoint will be used for the remainder analyses (n = 44, permutations = 999, pseudo-F = 0.305, $p = 0.784$).

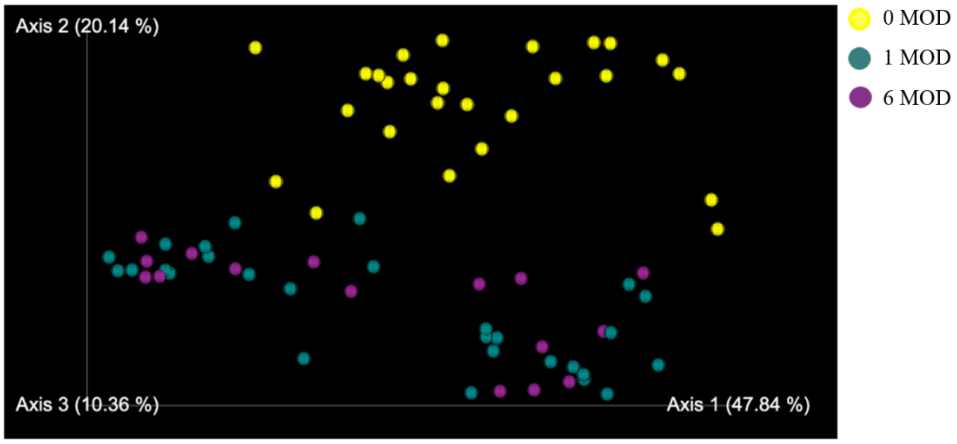

Figure 4. PCoA of weighted UniFrac distances according to month on diet in G1. A principal coordinate analysis (PCoA) plot of weighted UniFrac distances revealed overlap according to baseline condition (yellow dots) as well as overlap between 1 month (green dots) and 6 months (purple dots) on diet. No overlap was observed between baseline and 6 months on diet. Individual samples are represented by a dot.

3.2 Alpha Diversity within Parental Generation after 6 Months on Diet

After 6 months on experimental diet (6 MOD), there was a significant difference in mean Shannon diversity observed (H = 8.647, $p = 0.003$) wherein the MD had a significantly higher microbial diversity than the TAD. Similar trends were found when analyzing microbial richness measured through OTUs wherein the MD had significantly more OTUs observed after 6 MOD (H = 5.852, $p = 0.0156$) and microbial evenness measured through Simpson's evenness (H = 9.926, $p = 0.002$).

3.3 Beta Diversity within Parental Generation after 6 Months on Diet

When only examining 6 MOD to explore the differences caused by the comprehensive diets, there is no overlap between the two diet conditions, indicating a shift in the composition of the gut microbiome (Figure 5). PERMANOVA analysis determined the effects of 6 MOD on an experimental diet on the gut microbiome composition (n = 16, pseudo-F =29.474, $p = 0.002$) and indicated there is a statistically significant deviance in microbiome composition according to diet condition.

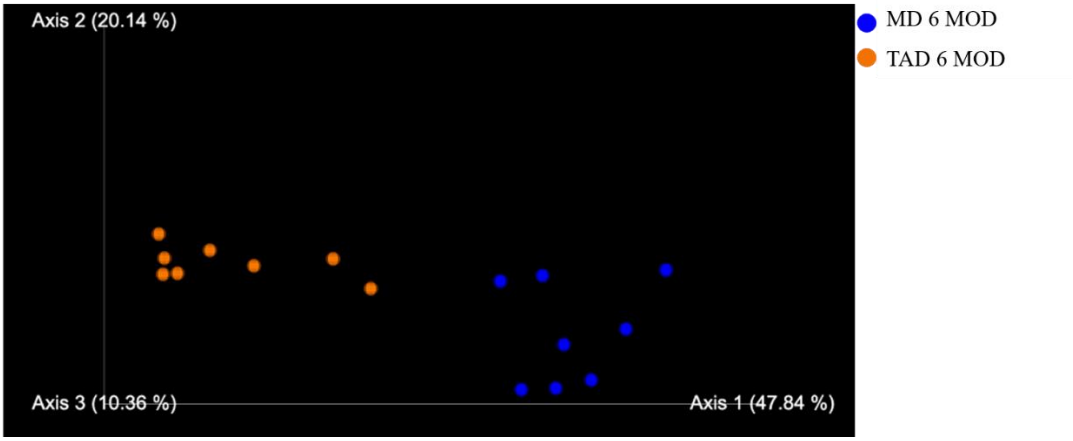

Figure 5. PCoA of weighted UniFrac distances according to diet condition in G1: 6 MOD. A principal coordinate analysis (PCoA) plot of weighted UniFrac distances revealed no overlap between animals after consuming either the MD or the TAD for 6 months. Individual samples are represented with a dot.

3.4 Taxonomic Analysis within Parental Generation after 6 Months on Diet

Differences in relative frequencies of taxonomies present due to diet condition were analyzed through taxa bar plots showing bacterial phyla and were supported by an unpaired t test

with Welch correction. Further analysis into specific differentially abundant bacteria was measured using an ANCOM test and related volcano plot.

Means of the relative frequencies of each sample in between diet condition were used to produce a taxa bar plot wherein phyla measured included Firmicutes, Verrucomicrobiota, Bacteroidetes, Proteobacteria, and Actinobacteria with all other present phyla grouped into an "Other" category. Taxa bar plots between the MD and TAD mice after 6 months on diet-TAD 6 MOD and MD 6 MOD, respectively-revealed differences in relative frequencies of bacterial phyla (Figure 6).

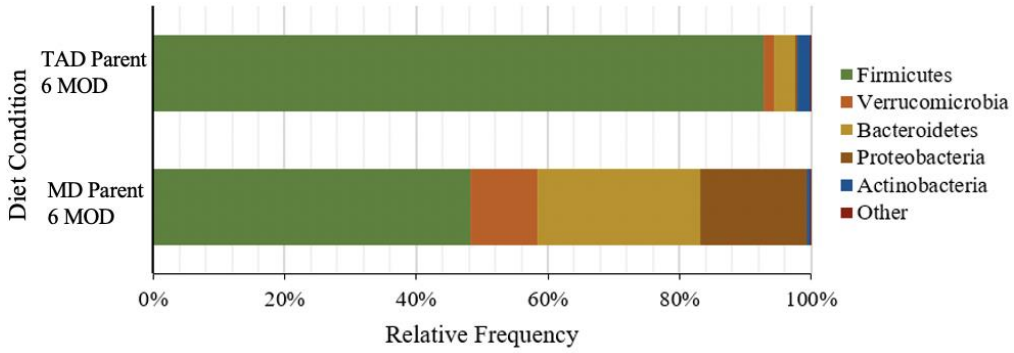

Figure 6. Taxa Bar Plots Examining Relative Frequency of Phyla in G1: 6 MOD. The mean relative frequencies from each diet condition after 6 months on diet were calculated to display the differentially present phylum in taxa bar plots. Different bacterial phyla are represented by different colors.

Multiple unpaired t-tests with Welch correction to account for inequal SD between groups were performed to analyze the statistical differences in relative frequencies between each phylum. Significant differences were found in all bacteria phyla, where mice consuming the MD for 6 months had a significantly elevated relative frequency of phyla Bacteroidetes, Proteobacteria, Verrucomicrobiota, and Actinobacteria and a lower relative frequency of

Firmicutes compared to the TAD (Table 2). Firmicutes were by far the dominant phyla within the TAD 6 MOD group, with the relative frequency being nearly double that found in the MD 6 MOD group.

Phylum	Mean of MD 6 MOD	Mean of TAD 6 MOD	*p*-value	SEM
Firmicutes	48.22%	92.82%	<0.001	6.011
Verrucomicrobiota	10.11%	1.52%	<0.001	2.258
Bacteroidetes	24.76%	3.17%	<0.001	2.462
Proteobacteria	16.29%	0.47%	<0.001	3.067
Actinobacteria	0.46%	1.87%	0.004	0.48

Table 2. Multiple Unpaired t-Tests of Phyla Relative Abundance Between Diet Condition in G1: 6 MOD. Mean relative abundance and standard deviations were calculated from raw data reported from the relative abundance taxa bar plot. An unpaired t-test was run to calculate the significance of difference between phyla after 6 months of experimental diet. N = 8.

Differential abundance on the genera level was analyzed using ANCOM volcano plots to examine the different supported bacteria after consuming a MD or TAD diet for 6 months. Analysis revealed 5 significantly differentially abundant bacteria genera (Figure 7). The TAD 6 MOD group showed a significant increase in abundance of genera within phyla Firmicutes- *Lactococcus*, *Lactobacillus*, and an unlisted genus in family *Peptostreptococcaceae*. The MD 6 MOD group had a significantly elevated abundance of *Sutterella* within the Proteobacteria phylum and *Clostridium* within the Firmicutes phylum. Analysis according to the species level was attempted, however due to limitations in the software's ability to provide identification down

to the species level, a majority of the differentially abundant species were unspecified further than genus. However, within the few species that were identified and deemed significant through unpaired t-tests, *Akkermansia muciniphilia* was significantly increased in the MD 6 MOD condition compared to the TAD 6 MOD condition (M MD = 6092.57, M TAD = 327.14, p =0.003).

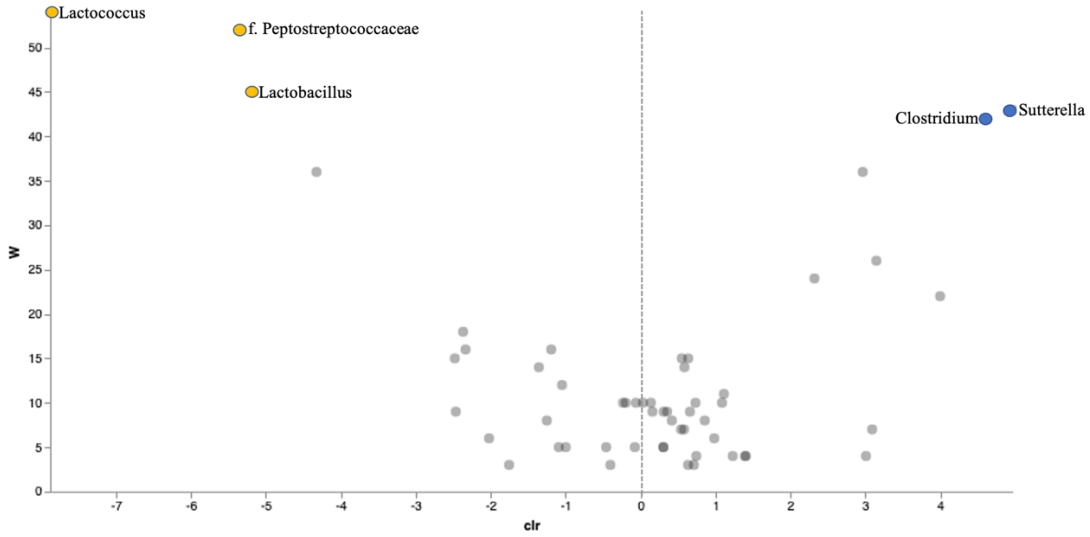

Figure 7. Labeled ANCOM Volcano Plot of Differentially Abundant Genera in G1: 6 MOD. An ANCOM test was run to generate a volcano plot displaying the reported differentially abundant bacterial genera according to diet condition. Bacteria genera significantly more abundant in the TAD are highlighted by a yellow dot and significantly more abundant bacteria genera in the MD are highlighted by a blue dot. Each individual dot represents a bacteria genus, with dots skewing away from 0 on the X-axis indicating difference in regulation and a higher W value indicating an increased significance of that difference in regulation. Top corners of the plot are ASVs suspected to be truly different across the groups. A predetermined W-value was used to determine significance through QIIME2 that is not available for the user.

3.5 Offspring Baseline and Parental Endpoint Microbial Similarities

Similarly to G1, offspring baseline (F1: 0 MOD) alpha diversity was measured using Shannon diversity, evenness through Simpson's evenness, and observed number of OTU's. A significant difference in Shannon diversity ($H = 7.456$, $p = 0.006$) according to experimental diet condition, reveals a higher community richness in baseline samples from in the MD group (F1: MD 0 MOD). A similar pattern was found when analyzing microbial evenness ($H = 7.456$, $p = 0.006$). Differences in beta diversity was examined using a PERMANOVA between diet conditions of F1: 0 MOD timepoint, revealing a significant difference between groups ($N = 16$, permutations = 999, pseudo-$F = 19.098$, $p = 0.001$).

As the F1: 0 MOD microbiome composition was hypothesized to be the same as the parental 6 MOD (G1: 6 MOD) composition within diet condition, alpha and beta diversity comparisons between the two generations according to diet condition were examined. Shannon diversity found no significant differences between the F1: TAD 0 MOD and the parental TAD 6 MOD (G1: TAD 6 MOD) ($H = 1.103$, $p = 0.294$) or the F1: MD 0 MOD and the parental MD 6 MOD (G1: MD 6 MOD) ($H = 2.482$, $p = 0.115$). Similar trends were found when examining Simpson's evenness for the TAD condition ($H = 0.069$, $p = 0.792$) or the MD condition ($H = 1.864$, $p = 0.172$).

As no significant differences in alpha diversity were observed when comparing G1: 6 MOD to F1: 0 MOD within either diet condition, there is no significant difference in community richness or evenness. However, a significant difference between beta diversity was observed and measured via a PERMANOVA within both the MD group ($N = 16$, permutations = 999, pseudo-$F = 5.417$, $p = 0.001$) and the TAD group ($N = 16$, permutations = 999, pseudo-$F = 3.982$, $p = 0.014$), indicating community composition differences. To further examine this, a taxa bar plot of

relative frequencies of bacteria phyla showed differences in the average values according to diet and generation (Figure 8).

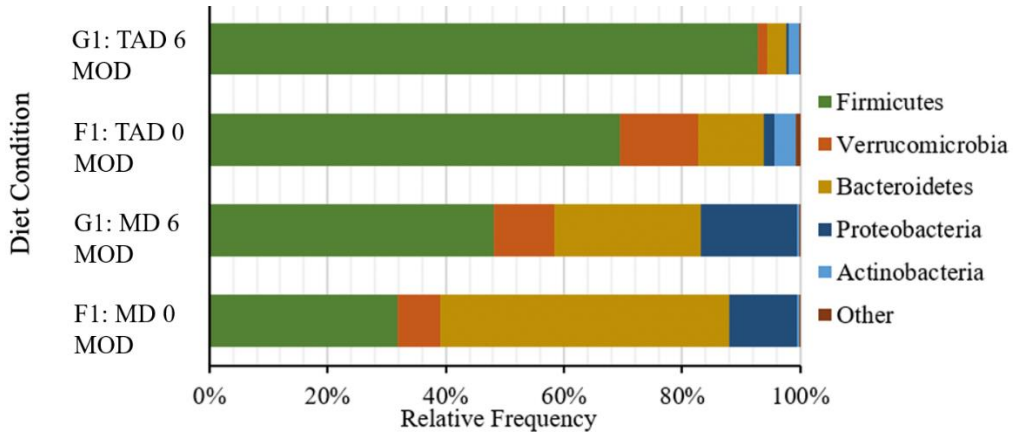

Figure 8. Taxa Bar Plots Examining Relative Frequency of Phyla Between F1: 0 MOD and G1: 6 MOD. The mean relative frequencies from each diet condition were calculated to display the differentially present phylum in taxa bar plots. Different bacterial phyla are represented by different colors.

Delving further into the differences in relative frequencies of bacteria phyla (Table 3), Firmicutes ($p = 0.003$, SEM = 5.489) had a significantly lower relative frequency in the F1: TAD 0 MOD than the G1: TAD 6 MOD. Additionally, Bacteroidetes were significantly higher ($p = 0.017$, SEM = 2.685) in the F1: TAD 0 MOD than the G1: TAD 6 MOD.

Table 3. Comparisons of Mean Relative Abundance of Bacterial Phyla Between G1: TAD 6 MOD and F1: TAD 0 MOD. Mean relative abundance and standard deviations were calculated from raw data reported from the relative abundance taxa bar plot. An unpaired t-test was run to calculate the significance of difference between phyla after parental consumption of the TAD for 6 months or the offspring baseline consumption of the TAD. N = 16.

Phylum	Mean of G1:TAD 6 MOD	Mean of F1:TAD 0 MOD	*p*-value	SEM
Firmicutes	92.82%	69.49%	0.003	5.849
Verrucomicrobiota	1.52%	13.31%	0.057	5.269
Bacteroidetes	3.16%	11.07%	0.017	2.685
Proteobacteria	0.47%	1.7%	0.063	0.590
Actinobacteria	1.88%	3.57%	0.119	0.996

Similar trends were found when looking at the offspring MOD 0 and parental MOD 6 samples that were within the MD condition (Table 4). Phylum Firmicutes were significantly lower in offspring MD 0 MOD samples ($p = 0.026$, SEM = 6.632) and phylum Bacteroidetes were significantly higher in offspring MD 0 MOD samples ($p = <0.001$, SEM = 4.947) compared to parental MD 6 MOD.

Table 4. Comparisons of Mean Relative Abundance of Bacterial Phyla Between G1: MD 6 MOD and F1: MD 0. Mean relative abundance and standard deviations were calculated from raw data reported from the relative abundance taxa bar plot. An unpaired t-test was run to calculate the significance of difference between phyla after parental consumption of the MD for 6 months or the offspring baseline consumption of the MD. N = 16.

Phylum	Mean of G1:MD 6 MOD	Mean of F1:MD 0 MOD	*p*-value	SEM
Firmicutes	48.21%	31.82%	0.026	6.632
Verrucomicrobiota	10.11%	7.35%	0.394	3.130

Bacteroidetes	24.76%	48.76%	<0.001	4.947
Proteobacteria	16.28%	11.44%	0.207	3.633
Actinobacteria	0.46%	0.36%	0.493	0.153

3.6 Offspring 2 Months on Diet and Parental Baseline Microbial Similarities

Offspring were fed standard rodent diet for 2 months, with their microbial communities hypothesized to shift to a shared composition. To examine this, alpha diversity was measured between the two offspring groups after transition to standard chow for 2 months (F1: 2 MOD) by examining Shannon diversity and Simpson's evenness. There were no significant difference in Shannon diversity ($H = 0.276$, $p = 0.600$) or Simpson's evenness ($H = 0.893$, $p = 0.345$) indicating no disparity in community diversity or evenness. A similar trend followed when examining the beta diversity of the two diet conditions after 2 MOD, with a PERMANOVA revealing no significant differences ($N = 16$, permutations = 999, pseudo-$F = 1.808$, $p = 0.201$). Due to these two similarities, there was no further downstream analysis comparing the two F1: 2 MOD groups.

As the G1: 0 MOD involves samples from mice still on standard rodent chow (prior to their weaning onto experimental diet) and the F1: 2 MOD also consume standard diet, the G1: 0 MOD and F1: 2 MOD samples were compared to examine similarities in microbial composition. Alpha diversity metrics revealed a significant difference between G1: 0 MOD and F1: 2 MOD when analyzing both the Shannon diversity metric ($H = 4.401$, $p = 0.0359$) and Simpson's evenness ($H = 4.401$, $p = 0.036$) wherein the F1 generation had higher diversity. A significant difference in beta diversity was also found through a PERMANOVA ($N = 42$, permutations = 999 pseudo-$F = 3.558$, $p = 0.015$). To further explore the disparity between these experimental

conditions, a taxa bar plot of average bacteria phyla relative frequency according to diet and generation was created (Figure 9).

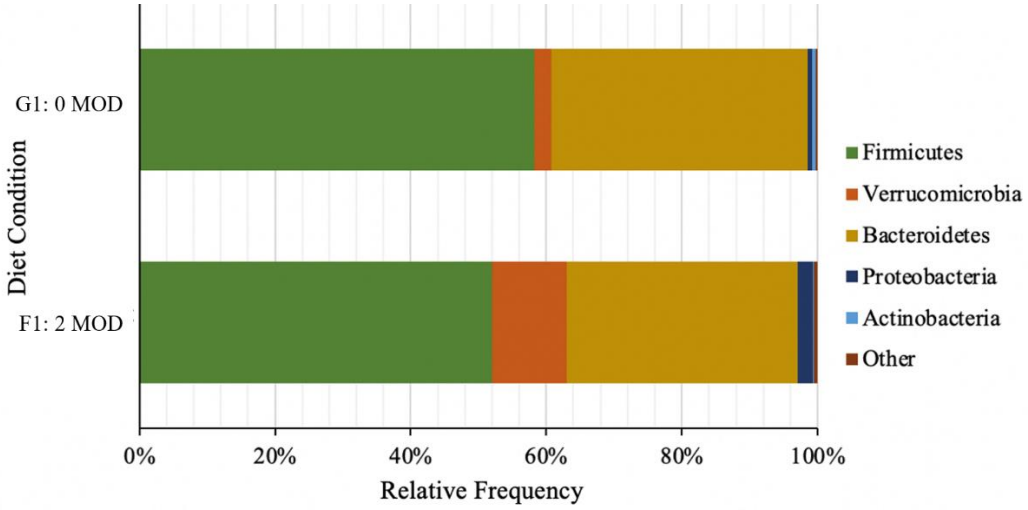

Figure 9. Relative Frequency Bar Plot of F1: 2 MOD and G1: 0 MOD. The mean relative frequencies from each diet condition were calculated to display the differentially present phylum in taxa bar plots. Different bacterial phyla are represented by different colors.

Unpaired t-tests were used to compare the average relative frequencies of each phylum between the F1: 2 MOD and the G1: 0 MOD. While the analyses revealed significant differences, these differences were within the two smallest bacterial phyla that combined make up between 1.22-2.24% of present bacterial phyla, thereby potentially limiting its significance to the study (Table 5).

Table 5. Comparisons of Mean Relative Abundance of Bacterial Phyla Between F1: 2 MOD and G1: 0 MOD. Mean relative abundance and standard deviations were calculated from raw data reported from the relative abundance taxa bar plot. An unpaired t-test was run to calculate the significance of different phyla between the offspring samples after standard diet for 2 months or parental baseline samples on standard diet. N = 42

Phylum	Mean of F1: 2 MOD	Mean of G1: 0 MOD	*p*-value	SEM
Firmicutes	52.00%	58.22%	0.363	3.31
Verrucomicrobiota	11.02%	2.55%	0.151	2.31
Bacteroidetes	34.07%	37.79%	0.450	2.61
Proteobacteria	2.29%	0.70%	0.020	0.28
Actinobacteria	0.12%	0.52%	0.006	0.09

DISCUSSION

The gut microbiome has been found to contribute to a wide variety of health and disease states, with the general composition and dominant species altering host energy and nutrient absorption, immune system function, and SCFA production (Kesika et al., 2021). While typically a decrease in alpha diversity and increase in pathogenic bacterial species is associated with disease, the exact bacterial composition associated with a specific disease state remains disputed. Alzheimer's disease is the most prevalent neurodegenerative disease, with several studies noting a trend in gut microbiome dysbiosis in patients with AD (Murray et al., 2022). Studies completed with AD patients have consistently found a decrease in both alpha diversity and beta diversity compared to healthy age-matched control populations (Heravi et al., 2023). Additionally, the impact of diet has been heavily implicated in the progression and risk of developing AD. Similarly, chronic consumption of a Western diet in rodents is associated with a decrease in both alpha and beta diversity compared to a standard diet control (Malesza et al., 2021). While there have been multiple studies exploring a Western diet or aspects of a Mediterranean diet in the lens of AD using mouse models, the comprehensiveness of previous studies are limited due to the composition of the experimental diets. For example, Western diets typically used in AD research have been comprised of 35-42% kcal fat and use a low-fat control diet of 10-15% kcal (Julien et

al., 2010; Pistell et al., 2010; Vogt et al., 2017) which is lower than the fat content present in a common human diet. In addition, the Mediterranean diets used in animal studies have been usually normal rodent chow supplemented with only one component of the Mediterranean diet, rather than a holistic diet (Garcia-Montero et al., 2021; Haskey et al., 2022). Therefore, our study utilized comprehensive diets with real-life macronutrient distributions and ingredients to compare its results to the currently existing literature with the main goal of increasing our capacity to translate results to humans.

To ensure sex was not a confounding variable within this study, beta diversity metrics were analyzed and revealed no sex differences. Therefore, male and female data was consolidated and analyzed together throughout the study. Baseline microbiome compositions were also confirmed to have no significant differences between experimental groups. The microbiome composition after 1 month on experimental diet and 6 months on experimental diet was compared to explore how fast the microbiome would shift and stabilize. We observed that the gut microbiome had completely shifted and stabilized to its final composition after only 1 MOD. Additionally, a significant difference in microbiome composition between the 0 MOD and 6 MOD suggested that the gut microbiome was significantly altered after 6 months of consuming either experimental diet condition. As the main focus of the study was to explore the effects of a long-term comprehensive, real-life diet on the gut microbiome in the lens of AD, only the 6 MOD timepoint within the parental generation was further explored.

As previously mentioned, an increase in alpha and beta diversity has been well established within AD and diet literature to indicate a healthier gut microbiome associated with several positive physiological effects (Heravi et al., 2023; Malesza et al., 2021). The initial hypothesis that consumption of the MD would lead to a higher alpha diversity compared to the consumption of the TAD was explored by comparing estimated richness and evenness to

examine the number of different species and the distribution of abundance between species, respectively. As predicted, consumption of the MD for 6 months lead to a significant increase in alpha diversity, indicating a healthier overall microbiome compared to the TAD experimental group's microbiome. Beta diversity was explored using weighted UniFrac distances and a PERMANOVA examined differences in community composition. The trends found, when comparing the MD group to the TAD group, the results followed those previously established in diet literature, with the MD group having higher beta diversity metrics compared to the TAD group after 6 months of diet consumption. These results also supported the MD group having a more diverse gut microbiome. These results led us to further explore the diversity at the phylum and genus level.

One limitation in the analysis of differentially abundant taxa associated with dysbiosis is inconsistent definitions across literature of what constitutes a microbiome in dysbiosis. Specifically, while both AD and a Western diet are commonly associated with a decrease in alpha and beta diversity, the differentially abundant phyla and genera responsible for disease development remains disputed. For instance, a 2022 systemic review analyzing the alterations in gut microbiome composition between AD patients and a healthy control population found that AD patients displayed a significant decrease in the phylum Firmicutes. Within this phylum, there was a significant increase of *Lactobacillus* and a significant decrease of *Sutterella* in AD patients (Murray et al., 2022). Contradicting these findings, a 2024 review analyzing AD and stage specific alterations of the gut microbiome found an increased level of Firmicutes in patients diagnosed with AD. Additionally, this study found that patients with mild cognitive impairment had a significantly higher abundance of *Sutterella,* with a positive correlation between *Sutterella* and increased Aβ burden. (Troci et al., 2024).

Analysis of the differences in mean relative abundance at phylum level between our TAD and MD groups revealed significant differences in several major phyla including Firmicutes, Verrucomicrobiota, Bacteroidetes, Proteobacteria, and Actinobacteria. A previous study utilizing these diets found phenotypic markers of AD after 6 months of consuming the TAD and protection from those markers in the MD group. It was hypothesized that the TAD group phyla distribution would represent that of an AD microbiome and the MD group phyla distribution would reflect a healthy controls' microbiome composition. The observed increase in the phylum Firmicutes and decrease in phylum Bacteroidetes found within the TAD group was also reported in some studies of AD patients' microbiomes (Troci et al., 2024). One potential explaination behind the nearly doubled relative abundance of Firmicutes (M TAD = 92.82%, M MD = 48.22%) and the significant decrease in Bacteroidetes in the TAD group is due to its fat source being predominantly animal fat. Previous studies using a high animal fat diet showed an abundance of Proteobacteria and Firmicutes, and a reduction in Bacteroidetes (Beam et al., 2021). However, the decrease of relative abundance of Proteobacteria within the TAD group was unexpected as it is typically a phylum associated with increased inflammation as found in the previous study using this diet (Beam et al., 2021).

In general, consumption of the diets led to the predicted gut microbiome diversities, but further analysis into specific taxa becomes more complex as the relevant literature is not uniform in its findings. Differential abundance of bacterial genera according to diet condition after 6 months on diet was explored using an ANCOM volcano plot. The results showed 5 differentially abundant taxa, with 3 genera increased in the TAD group and 2 genera increased in the MD group. The initial hypothesis of inflammatory bacteria being more abundant in the TAD and probiotic bacteria being more abundant in the MD was not supported by downstream analyses. For example, the TAD group had a significantly higher relative abundance of genus *Lactococcus*.

However, an increase in *Lactococcus* species is not associated with the consumption of a high fat Western diet or AD. Rather, it is considered the most important probiotic genera of the gut microbiome and is implicated in maintaining mucosal barrier defenses and promoting the anti-inflammatory response. *Lactococcus* has been shown help mitigate symptoms associated with AD and the low-grade inflammation from obesity caused by a Western diet (Rastogi & Singh, 2022). While *Lactococcus* is mainly found through consumption of dairy and fermented food, one possible explanation of this unexpected increase within the TAD group is the consumption of casein can significantly increase the abundance of some *Lactococcus* species (Zhao et al., 2019). Specifically, the MD formulation contains 0 grams/Kg of casein, while the TAD formulation contains 165.5 grams/Kg of casein (Appendix D). A standard rodent diet, which is typically used as a control in high-fat diet studies, contains a similar level of casein to the TAD at 200 grams of casein, which also may explain the lack of differential abundance of *Lactococcus* in high fat Western diet studies (Braden-Khule, 2024). Similarly, a significant increase of *Lactobacillus* in the TAD group was found, but there are disparities with the potential benefit in AD. While *Lactobacillus* is a probiotic genus that has led to improved cognition in AD patients, some studies have found an increase of *Lactobacillus* in AD patients (Lyte, 2011; Murray et al., 2022; Vogt et al., 2017). The family *Peptostreptococcaceae* was also upregulated in the TAD group, however limitations in data analysis produced no breakdown of its 15 genera and therefore the significance of this finding is unknown (Bello et al., 2024). Within the MD group, genera *Clostridium* and *Sutterella* were increased compared to the TAD group after 6 months on diet. While the abundance of genera *Clostridium* has been found to be significantly increased following consumption of an animal-protein based diet, contrastingly, it has also been found to be significantly decreased both in AD patient's microbiomes or following the consumption of a Mediterranean diet (Beam et al., 2021; Murray et al., 2022; Singh et al., 2017). Genera

Sutterella was also significantly more abundant in the MD group. The significance of this genera also has been disputed in literature as some studies report a decrease in abundance in AD patients, while others report not only an increase of abundance in AD patients, but also a positive association with *Sutterella* and increased amyloid beta burden (Murray et al., 2022; Troci et al., 2024). While the significantly differentially abundant bacteria found within this study generally contradicts what has been found in established literature, further analysis into the responsible species driving the differentially abundances would have led to stronger conclusions. However, limitations in data analysis prevented consistent identifications of bacterial species.

A secondary component to this study was the initial and lasting effect of experimental perinatal diet on offspring microbial composition. As initial microbial colonization occurs from maternal exposure (Mackie et al., 1999), we hypothesized that the offspring baseline microbiome compositions would not be significantly different than that of the parent after 6 months on diet. Results revealed no significant differences in alpha diversity metrics comparing F1: 0 MOD samples to G1: 6 MOD samples within the TAD group and the MD group, supporting our hypothesis. As expected, comparisons of the F1: MD 0 MOD to F1: TAD 0 MOD also revealed similar trends found in the parental 6 month on diet analysis wherein the MD group had significantly higher alpha diversity metrics than the TAD group. However, there was a significant difference in beta diversity metrics within either diet condition when comparing F1: 0 MOD samples to G1: 6 MOD samples. Previous studies have contradicting results wherein the microbial composition of children during their first year of life had a higher alpha diversity and lower beta diversity compared to their mothers (Backhed et al., 2015). Further unpacking this difference through analyzing relative frequencies of phyla according to diet condition and generation revealed a general trend wherein the offspring samples had a significantly lower frequency of Firmicutes and a significantly higher frequency of Bacteroidetes, regardless of diet

condition. Contrasting to these results, studies comparing children's microbial composition to adults found a similar distribution of Firmicutes across age, but that Bacteroidetes were significantly more abundant in adults than children between 1-4 years old (Ringel-Kulka et al., 2013). While different abundant bacteria are noted between neonates and adults due to a still shifting microbiome, the specific phyla differences reported depend on several confounding factors in studies including method of delivery, environmental exposures, age of weaning, placental bacterial exposure, and diet (Meropol & Edwards, 2015).

While we had previously established that the gut microbiome fully shifted after 1 month on diet to a stable microbiome that was also found after 6 months on diet, the long-lasting effects of perinatal diet condition was explored by transitioning both offspring experimental diet groups to a standard diet for 2 months. Early microbial composition is vital for training and development of the immune system, with potential long-lasting consequences of an irreversibly differentially developed immune system (El Aidy et al., 2013; Mackie et al., 1999). Comparisons of alpha and beta diversity between offspring diet groups after 2 months on standard diet revealed no significant differences based on perinatal diet condition. Parental baseline condition samples wherein the animals were on standard diet was compared to offspring samples after 2 months on standard diet to see if the microbiomes had fully shifted to the original composition. There were significant differences in both alpha and beta diversity, wherein the offspring had higher diversity. Unpaired t-tests found the phyla that Proteobacteria and Actinobacteria phyla had significantly different relative frequency, with both phyla combined only making up between 1.22-2.24% of the bacterial phyla present. While an age-matched, standard diet control would have served as a better standard diet representative, the differences in the reported phyla have limited major translational effects on the health of the overall microbiome.

LIMITATIONS AND FUTURE DIRECTIONS

A number of limitations to our study were uncovered and will need to be addressed in the future. Due to the sheer number of dependent variables investigated in the initial study, of which the microbiome was just one, a coordinated effort of many undergraduate and graduate students was required. Collecting the microbiome was not originally a main focus of the project, but funding became available to pursue this avenue and thus we proceeded to collect microbiome, with no previous experience. Below we list several limitations to our study and how they will be addressed in future microbiome studies within the constraints of TCU's vivarium.

Sanitation

Sterility is vital when conducting a gut microbiome study as introduction of extraneous bacteria can lead to contaminated samples and incorrect data. This is especially important when comparing two experimental groups as shared exposure of environment can lead to cross-contamination. There were multiple points in this study where cross-contamination due to animal handling could have and likely did occur. The mice were stored in the vivarium under sanitary conditions, but no additional procedures were implemented to limit cross-contamination between cages or diet conditions.

Animal Handling

If cross contamination did occur, one likely reason would be that students working with animals did not change gloves between cages or diet conditions. Buckets were used for collecting weekly body weight measurements and food consumption levels, with a different bucket for each diet condition. No sanitation methods were implemented between cages, thereby possibly introducing microbes from different cages to the same shared environment. After

measurements, sanitation of these buckets often only included rinsing with water and storage on an uncleaned shared drying rack. Animals were housed in non-ventilated cages, primarily for acclimating to the environment for the main study's behavioral paradigms. This shared exposure to room air may also have added to the environmental microbe exposure and potential cross-contamination.

In future studies of gut microbiome, we are implementing a strict sanitation policy when handling the animals. Gloves will be sanitized using Quadratop when handling cages/animals across cages but within the same diet condition, and a glove change is required when handling cages/animals within different diet conditions. All body and food weight measurements will take place in cups that are sanitized and not reused between cages or diet conditions to limit cross-contamination. Additionally, for the duration of the microbiome aspect of the study, animals will be housed in ventilated cages and handled as minimally as possible.

Sample Handling

While indirect exposure of microbes possibly occurred when handling animals throughout this study, there was also a small amount of direct exposure of microbes from one collected fecal sample to the next. Materials used during fecal sample collection – holding cages and tweezers – were re-used across all samples. Mice were placed in a separate holding cage while waiting for them to drop fecal samples, and thus they would explore and urinate in the holding cages. Often students would re-use the holding cage between animals and we could not be sure that the cages were cleaned between each animal. In addition, only one pair of un-sanitized serrated tweezers were used to pick up all fecal pellets with no cleaning in-between collections. To address this limitation in the future, animals will be assigned an individual cage that will not be re-used

during collection and autoclaved toothpicks will be used to pick up fecal samples that will be immediately frozen in dry ice.

Sample Errors

This study utilized many undergraduate students to collect the large number of samples at many timepoints. There was not a standardized labeling method on the sample tubes leading to difficulty in grouping samples for analysis, or blatant mislabeling of samples, and even samples being misplaced in freezer boxes. The main issue was that students were not consistent in labeling tubes with the appropriate timepoint. Some students labeled the samples with the mouse's age in months at the time the sample was collected or they labeled the tubes with the months the mouse was on diet. Thus, when opening a box of tubes that were supposed to be from animals that had been on diet for 1month, there were tubes also labeled 2 (which could have meant 2 month-old mice or 2 months on diet. As there was no master list of all samples collected at all timepoints, we had to retroactively go back to try and sort out which samples were baseline or experimental, with many samples excluded from analysis due to a lack of discernible date or no baseline provided. A lack of master list also limited the ability to perform a longitudinal study as many samples did not have more than 1 or 2 samples collected that we were confident in the collection timepoint. This led to an extremely limited sample size for downstream analysis and some samples as outliers. As undergraduates were primarily used to collect fecal pellets, there were also multiple instances where proper identification of animals within a cage was incorrect, or animals were temporarily put back into the wrong home cage, causing the confidence in accurate sampling to be limited. For future studies, all sample vials and boxes will be labeled using a standardized system to prevent any miscommunication of sample components. Additionally, all sample collection is being overseen by a graduate student and only

one undergraduate. Less timepoints are being collected to ease the burden on the associated students and to ensure that a longitudinal study can be performed.

Timing

Timing of collection has been well established to drastically change the composition of the gut microbiome depending on timing of last meal and time of day. However, time of sample collection throughout our study varied greatly from early morning to the evening leading to inconsistent collection parameters. The F1 generation specifically was limited because of the already small sample size. This study combined 2 months and 3 months on diet for F1 so the data could still be analyzed, but this is an incorrect method of interpreting results. For the future studies, collections will occur at 7am each time and at the same age for all animals. To make this a viable alteration, animals were split into smaller batches within the study.

Future Studies

Initial data analysis using QIIME2 allowed for basic data analysis in a predominately user-friendly based format. However, because this was our first experience with performing microbiome analysis, we found issues determining what tests could be performed using QIIME2, and that often the statistical parameters chosen by QIIME2 were not reported, which led us to wonder if another data analysis format should be used. For instance, while there were several reported differentially abundant species in the ANCOM plot, analysis of the raw abundances from the taxa bar plots suggest additional genera may be differentially abundant as well, but this information was not available in QIIME2.

In addition to repeating the current study with stricter parameters as listed above, all future studies will include measuring SCFA metabolites directly from serum as several metabolites

have known beneficial or detrimental qualities and alterations in production is associated with different diet conditions. Further alterations to either experimental diet could also strengthen the research. For instance, the addition of plant polyphenols and more diverse fiber sources to the MD could increase the translatability to human diet, and the addition of more diverse fat types and representative soluble fiber sources to the TAD would increase its comprehensiveness.

APPENDICES

Appendix A: Methodology

MagMAX_Microbiome_Stool_Flex protocol

MagMAX_Microbiome_Stool_Flex: started; Tip1: started; Temperature: 20 °C

Tip1: Plate 'Tip Comb Plate' loaded with 96 DW tip comb.

Binding: started; Temperature: 20 °C

11 Minutes of Binding: completed

11 Minutes of Collect_Beads: started; Temperature: 20 °C

Collect_Beads: completed

Wash 1: started; Temperature: 20 °C

11 Minutes of Wash 1: completed

Wash 2: started; Temperature: 20 °C

11 Minutes of Wash 2: completed

Wash 3: started; Temperature: 20 °C

11 Minutes of Wash 3: completed

Wash 4: started; Temperature: 75 °C

11 Minutes of Wash 4: completed

Dry: started; Temperature: 75 °C

3 Minutes of Dry: completed

Elution: started; Temperature: 75 °C

5 Minutes of Elution: completed

Collect Beads: started; Temperature: 10 °C

Collect Beads: completed; Tip1: completed

MagMAX_Microbiome_Stool_Flex: completed

Appendix B: Terminology Dictionary

Methodology and Results

- Amplicon PCR – Type of PCR that amplifies the V4 region of interest using specific primers with overhang adapters attached
- Cluster Generation – The process where fragments of nucleic acids are clustered on the solid surface of the flow cell in preparation for sequencing which allows later identification and characterization of microbial communities
- Index PCR – This step attaches dual indices and sequencing adapters thereby giving each sample a known barcode for later identification

- Library Pooling – Combining different libraries allows for multiple samples to be run at the same time, thereby saving time, money, and helps normalize samples. The samples are able to be pooled as they were given a unique barcode at the index PCR step
- PCR Cleanup – Essential step that purifies the sample from free primers and primer dimer species
- V4 primers – specific primers that target the V4 region of the 16S rRNA gene in bacteria. This region has both conserved regions that are used to classify according to species and variable regions that are used for downstream classification

Results

- Alpha Diversity – Mean diversity of species and microbial diversity within each sample. Beta Diversity – Measures similarity or dissimilarity between two communities
- Evenness - Measurement of alpha diversity, measurement of distribution of abundances of organisms within each sample
- Measurements include looking at the richness and evenness within a sample
- OTU (Operational Taxonomic Units) – Based on sequence similarity in a specific part of a gene, OTUs represent related groups, with more OTUS present indicating a higher level of diversity. Within QIIME2, the threshold for the sequence similarity threshold that defines an OTU was 97% similarity. This number was used as it usually corresponds to identification on the species level in bacteria
- PCoA (Principle Coordinate Analysis) – measures based on distance rather than variation, so it preserves distances generated from dissimilarity measures when looking at beta diversity. More similar subjects are in overlapping grouping. The PCoA transforms a

multigenerational matrix to a new set of axes, with a successful PCoA generating axes with large eigen values that capture above 50% of data variation

- PERMANOVA – Tests where distances between samples within a group are more similar to each other than samples from a different group
- Phylogenetic relationship – The relationships between organisms throughout evolution as found by comparing observed heritable traits
- Shannon Diversity Index – Measurement of alpha diversity, quantitative measurement of community richness by looking at the different number of taxonomic groups within each sample
- Weighted UniFrac – A quantitative measure of community dissimilarity that incorporates phylogenetic relationships between features. It analyzes beta diversity through measuring the evolution within each community by using the branch length of a phylogenetic tree, with a weighted UniFrac weighted by difference in probability of mass of OTUs from each community branch. Therefore, it detects community differences that arise form differences in relative abundance of taxa, rather than which taxa are present

Coding

- Artifacts (.qza) – results that are an intermediate in data analysis. It is generated by QIIME2 and intended to be consumed by QIIME2. Can eventually be used to produce a visualization
- Demultiplexing data – Demultiplexing involves assigning the sequences to the sample they are derived from thereby separating out each sample from the pooled library
- Denoising – A quality control step in DADA2 that performs quality filtering, chimera checking, and paired end read joining. Chimeras form from two or more sequences

merging together during the sequencing process. Paired end read joining is necessary for further analysis as it joins the forward sequence to the reverse sequence for each sample

- FASTQ files – Raw sequence file that stores nucleotide sequences and the related quality scores
- Feature Table – Contains counts (frequencies) of each unique sequence in each sample in the dataset and maps the feature identifiers to the sequences they represent. It can give you information on how many sequences are associated with each samples, histograms of distributions, and related summary statistics
- Naïve Bayes Classifier – Pre-trained classifier that was trained on the Greengenes 13_8 99% OTUs where this will generate a visualization of sample sequences to taxonomy that share 99% similarity in OTUs
- Pipeline – A type of action in QIIME2 that combines two or more actions, so it can take one or more inputs and produce one or more results
- Plugin – Provides an analysis functionality
- Rooted Tree – Downstream metrics of phylogenetic diversity require a rooted phylogenetic tree to related the features to one another. The sequences are aligned, then filtered to remove highly variable features, then applies FastTree to generate a phylogenetic tree. FastTree creates an unrooted tree, which is then converted to a rooted tree by midpoint rooting
- Visualizations (.qzv) – QIIME2 results that represent terminal output in analysis. They are produced by QIIME2 and intended to be consumed by a human. Visualizations can be viewed by the code “qiime tools view <.qzv file>”

Appendix C: Coding Inputs and Outputs

Key:

Black Font – Descriptions

Red Font – Input

Blue Font – Artifacts

Green Font – Visualizations

Installation

Installing Miniconda3 macOS Intel x86 64-bit bash

Download from website link and dragged to personal file (viviennelacy)

Within terminal window

bash Miniconda3-latest-MacOSX-x86_64.sh

Followed prompts, then closed and reopened file

conda list

Files of Miniconda3 should pop up

Installing QIIME2 Natively

Update Miniconda3

conda update conda

Install wget

conda install wget

Install QIIME2 with conda environment – amplicon distribution

wget https://data.qiime2.org/distro/amplicon/qiime2-amplicon-2023.9-py38-osx-conda.yml

conda env create -n qiime2-amplicon-2023.9 –file qiime2-amplicon-2023.9-py38-osx-conda.yml

Activate conda environment

conda activate qiime2-amplicon-2023.9

Test environment is open and being used

qiime –help

To reactivate qiime2 environment

conda activate qiime2-amplicon-2023.9

All QIIME2 visualizations can be view using

qiime tools view <nameoffile.qzv>

Importing Raw Data Files

Make new directory

mkdir unt-data

cd unt-data

Upload data

qiime tools import \

--type ‘SampleData[PairedEndSequencesWithQuality]’ \

--input-path “/Volumes/Seagate Expansions Drive/UNT_Microbiome” \

--input-format CasavaOneEightSingleLanePerSampleDirFmt \

--output-path demux-paired-end.qza

Output artifact:

demux-paired-end.qza

Denoising and Generating Feature Table

This step results in artifacts including the feature table, corresponding feature sequences, and DADA2 denoising stats for quality. The DADA2 pipeline also pairs end sequences.

qiime demux summarize \

--i-data demux-paired-end.qza \

--o-visualization demux.qzv

qiime dada2 denoise-paired \

--i-demultiplexed-seqs demux-paired-end.qza

--p-trim-left-f 10 \

--p-trim-left-r 10 \

--p-trunc-len-f 210 \

--p-trunc-len-r 210 \

--o-table table.qza \

--o-representative-sequences rep-seqs.qza \

--o-denoising-stats denoising-stats.qza

Outputs artifacts:

table.qza

rep-seqs.qza

denoising-stats.qza

Adding and Tabulating Metadata

Make a metadata file that includes the sample ID that matches the sample ID from the raw data sequences. Additional information such as grouping conditions can be added at this time then filtered down in downstream analysis. The table created in this step will be used as the main source of data for further analysis. Checking denoising stats will also give quality scores if low quality samples need to be filtered out.

Check the file was present in the path being used

ls "/Users/viviennelacy/Desktop/d"

Output visualization:

QIIMEmeta.tsv

Tabulate metadata

```
qiime metadata tabulate \
  --m-input-file "/Users/viviennelacy/Desktop/d/QIIMEmeta.tsv" \
  --o-visualization tabulated-sample-metadata.tsv
```

Output visualization:

tabulated-sample-metadata.tsv

```
qiime feature-table summarize \
  --i-table table.qza
  --o-visualization table.qzv \
  -m-sample-metadata-file “/Users/viviennelacy/Desktop/d/QIIMEmeta.tsv”
```

Output visualization:

table.qzv

```
qiime feature-table tabulate-seqs \
  --i-data rep-seqs.qza
  --o-visualization rep-seqs.qzv
```

Output visualization:

rep-seqs.qsv

```
qiime metadata tabulate \
  --m-input-file denoising-stats.qza \
  --o-visualization denoising-stats.qzv
```

Output visualization:

denoising-stats.qzv

Identifying Phylogeny

Create a phylogenetic tree

```
qiime phylogeny align-to-tree-mafft-fasttree \
  --i-sequences rep-seqs.qza \
  --o-alignment aligned-rep-seqs.qza \
  --o-masked-alignment masked-aligned-rep-seqs.qza \
  --o-tree unrooted-tree.qza \
  --o-rooted-tree rooted-tree.qza
```

Output visualization:

aligned-rep-seqs.qza

masked-algined-rep-seqs.qza

rooted-tree.qza

unrooted-tree.qza

Use a classifier to identify species and reclassify taxonomy

```
wget \
  -O "gg-13-8-99-515-806-nb-classifier.qza" \
```

```
  https://data.qiime2.org/2023.9/common/gg-13-8-99-515-806-nb-classifier.qza

qiime feature-classifier classify-sklearn \

  --i-classifier gg-13-8-99-515-806-nb-classifier.qza \

  --i-reads rep-seqs.qza \

  --o-classification taxonomy.qza

qiime metadata tabulate \

 --m-input-file taxonomy.qza \

 --o-visualization taxonomy.qzv

qiime metadata tabulate \

  --m-input-file taxonomy.qza \

  --o-visualization taxonomy.qzv
```

Output Visualization:

taxonomy.qzv

Differential Abundance Testing – Parental Generation

Create Feature Table

```
qiime feature-table filter-samples \

  --i-table table.qza \

  --m-metadata-file "/Users/viviennelacy/Desktop/d/QIIMEmeta.tsv" \
```

--p-where "[genmod]='G1'" \

--o-filtered-table G1-table.qza

Output Artifact:

G1-table.qza

qiime composition add-pseudocount \

--i-table G1-table.qza \

--o-composition-table comp-G1-table.qza

Output Artifact:

Comp-G1-table.qza

Looking at diet

qiime composition ancom \

--i-table comp-G1-table.qza \

--m-metadata-file "/Users/viviennelacy/Desktop/d/QIIMEmeta.tsv" \

--m-metadata-column diet \

--o-visualization ancom-G1-diet.qzv

Output Visualization:

ancom-G1-diet.qzv

Look at genus level

qiime taxa collapse \

```
  --i-table G1-table.qza \
  --i-taxonomy taxonomy.qza \
  --p-level 6 \
  --o-collapsed-table G1-diet-l6.qza
```

Output Artifact:

G1-diet-l6.qza

```
qiime composition add-pseudocount \
  --i-table G1-diet-l6.qza \
  --o-composition-table comp-G1-diet-table-l6.qza
```

Output Artifact:

comp-G1-diet-table-l6.qza

```
qiime composition ancom \
  --i-table comp-G1-diet-table-l6.qza \
  --m-metadata-file "/Users/viviennelacy/Desktop/d/QIIMEmeta.tsv" \
  --m-metadata-column diet \
 --o-visualization l6-ancom-G1-diet.qzv
```

Output Visualization:

l6-ancom-G1-diet.qzv

G1 Analysis

Filter the metadata table

```
qiime feature-table filter-samples \
  --i-table table.qza \
  --m-metadata-file "/Users/viviennelacy/Desktop/parent/gandfmeta.tsv" \
  --p-where "[genmod]='G'" \
  --o-filtered-table parent-table.qza
```

Output Artifact:

parent-table.qza

Alpha and beta diversity core metrics

```
qiime diversity core-metrics-phylogenetic \
  --i-phylogeny rooted-tree.qza \
  --i-table parent-table.qza \
  --p-sampling-depth 115 \
  --m-metadata-file "/Users/viviennelacy/Desktop/parent/gandfmeta.tsv" \
  --output-dir gandf-core-metrics-results
```

Output Artifacts:

Saved FeatureTable[Frequency] to: gandf-core-metrics-results/rarefied_table.qza

Saved SampleData[AlphaDiversity] to: gandf-core-metrics-results/faith_pd_vector.qza

Saved SampleData[AlphaDiversity] to: gandf-core-metrics-results/observed_features_vector.qza

Saved SampleData[AlphaDiversity] to: gandf-core-metrics-results/shannon_vector.qza

Saved SampleData[AlphaDiversity] to: gandf-core-metrics-results/evenness_vector.qza

Saved DistanceMatrix to: gandf-core-metrics-results/unweighted_unifrac_distance_matrix.qza

Saved DistanceMatrix to: gandf-core-metrics-results/weighted_unifrac_distance_matrix.qza

Saved DistanceMatrix to: gandf-core-metrics-results/jaccard_distance_matrix.qza

Saved DistanceMatrix to: gandf-core-metrics-results/bray_curtis_distance_matrix.qza

Saved PCoAResults to: gandf-core-metrics-results/unweighted_unifrac_pcoa_results.qza

Saved PCoAResults to: gandf-core-metrics-results/weighted_unifrac_pcoa_results.qza

Saved PCoAResults to: gandf-core-metrics-results/jaccard_pcoa_results.qza

Saved PCoAResults to: gandf-core-metrics-results/bray_curtis_pcoa_results.qza

Output Visualizations:

Saved Visualization to: gandf-core-metrics-results/unweighted_unifrac_emperor.qzv

Saved Visualization to: gandf-core-metrics-results/weighted_unifrac_emperor.qzv

Saved Visualization to: gandf-core-metrics-results/jaccard_emperor.qzv

Saved Visualization to: gandf-core-metrics-results/bray_curtis_emperor.qzv

Alpha diversity in the context of metadata

Simpson's Evenness

```
qiime diversity alpha-group-significance \
  --i-alpha-diversity gandf-core-metrics-results/evenness_vector.qza \
  --m-metadata-file "/Users/viviennelacy/Desktop/parent/gandfmeta.tsv" \
  --o-visualization gandf-core-metrics-results/evenness-group-significance.qzv
```

Output Visualization:

gandf-core-metrics-results/evenness-group-significance.qzv

Shannon Index

```
qiime diversity alpha-group-significance \
  --i-alpha-diversity gandf-core-metrics-results/shannon_vector.qza \
  --m-metadata-file "/Users/viviennelacy/Desktop/parent/gandfmeta.tsv" \
  --o-visualization gandf-core-metrics-results/shannon-vector-group-significance.qzv
```

Output Visualization:

gandf-core-metrics-results/shannon-vector-group-significance.qzv

Observed features:

```
qiime diversity alpha-group-significance \
  --i-alpha-diversity gandf-core-metrics-results/observed_features_vector.qza \
  --m-metadata-file "/Users/viviennelacy/Desktop/parent/gandfmeta.tsv" \
  --o-visualization gandf-core-metrics-results/observed-features-group-significance.qzv
```

Output Visualization:

gandf-core-metrics-results/observed-features-group-significance.qzv

Beta diversity in the context of metadata

The effect of months on diet

```
qiime diversity beta-group-significance \
  --i-distance-matrix gandf-core-metrics-results/weighted_unifrac_distance_matrix.qza \
  --m-metadata-file "/Users/viviennelacy/Desktop/parent/gandfmeta.tsv" \
  --m-metadata-column mod \
  --o-visualization gandf-core-metrics-results/weighted-unifrac-mod-significance.qzv \
  --p-pairwise
```

Output Visualization:

gandf-core-metrics-results/weighted-unifrac-mod-significance.qzv

The effects of diet condition

```
qiime diversity beta-group-significance \
   --i-distance-matrix gandf-core-metrics-results/weighted_unifrac_distance_matrix.qza \
   --m-metadata-file "/Users/viviennelacy/Desktop/parent/gandfmeta.tsv" \
  --m-metadata-column diet \
   --o-visualization gandf-core-metrics-results/weighted-unifrac-diet-significance.qzv \
```

```
  --p-pairwise
```

Output Visualization:

gandf-core-metrics-results/weighted-unifrac-diet-significance.qzv

The effects of sex

```
qiime diversity beta-group-significance \
    --i-distance-matrix gandf-core-metrics-results/weighted_unifrac_distance_matrix.qza \
    --m-metadata-file "/Users/viviennelacy/Desktop/parent/gandfmeta.tsv" \
   --m-metadata-column sex \
    --o-visualization gandf-core-metrics-results/weighted-unifrac-sex-significance.qzv \
  --p-pairwise
```

Output Visualization:

gandf-core-metrics-results/weighted-unifrac-sex-significance.qzv

G1: 6 MOD

Feature table

```
qiime feature-table filter-samples \
  --i-table parent-table.qza \
  --m-metadata-file "/Users/viviennelacy/Desktop/parent/gandfmeta.tsv" \
  --p-where "[mod]='6'" \
```

--o-filtered-table G6-analysis-table.qza

Output Artifact:

G6-analysis-table.qza

Alpha and beta diversity core metrics after 6 months on diet

```
qiime diversity core-metrics-phylogenetic \
 --i-phylogeny rooted-tree.qza \
 --i-table G6-analysis-table.qza \
 --p-sampling-depth 115 \
 --m-metadata-file "/Users/viviennelacy/Desktop/parent/gandfmeta.tsv" \
 --output-dir g6-core-metrics-results
```

Output Artifacts:

Saved FeatureTable[Frequency] to: g6-core-metrics-results/rarefied_table.qza

Saved SampleData[AlphaDiversity] to: g6-core-metrics-results/faith_pd_vector.qza

Saved SampleData[AlphaDiversity] to: g6-core-metrics-results/observed_features_vector.qza

Saved SampleData[AlphaDiversity] to: g6-core-metrics-results/shannon_vector.qza

Saved SampleData[AlphaDiversity] to: g6-core-metrics-results/evenness_vector.qza

Saved DistanceMatrix to: g6-core-metrics-results/unweighted_unifrac_distance_matrix.qza

Saved DistanceMatrix to: g6-core-metrics-results/weighted_unifrac_distance_matrix.qza

Saved DistanceMatrix to: g6-core-metrics-results/jaccard_distance_matrix.qza

Saved DistanceMatrix to: g6-core-metrics-results/bray_curtis_distance_matrix.qza

Saved PCoAResults to: g6-core-metrics-results/unweighted_unifrac_pcoa_results.qza

Saved PCoAResults to: g6-core-metrics-results/weighted_unifrac_pcoa_results.qza

Saved PCoAResults to: g6-core-metrics-results/jaccard_pcoa_results.qza

Saved PCoAResults to: g6-core-metrics-results/bray_curtis_pcoa_results.qza

Output Visualization:

Saved Visualization to: g6-core-metrics-results/unweighted_unifrac_emperor.qzv

Saved Visualization to: g6-core-metrics-results/weighted_unifrac_emperor.qzv

Saved Visualization to: g6-core-metrics-results/jaccard_emperor.qzv

Saved Visualization to: g6-core-metrics-results/bray_curtis_emperor.qzv

Alpha diversity in context of metadata:

Evenness

```
qiime diversity alpha-group-significance \
  --i-alpha-diversity g6-core-metrics-results/evenness_vector.qza \
  --m-metadata-file "/Users/viviennelacy/Desktop/parent/gandfmeta.tsv" \
  --o-visualization g6-core-metrics-results/evenness-group-significance.qzv
```

Output Visualization:

g6-core-metrics-results/evenness-group-significance.qzv

Shannon index

```
qiime diversity alpha-group-significance \
  --i-alpha-diversity g6-core-metrics-results/shannon_vector.qza \
  --m-metadata-file "/Users/viviennelacy/Desktop/parent/gandfmeta.tsv" \
  --o-visualization g6-core-metrics-results/shannon-vector-group-significance.qzv
```

Output Visualization:

g6-core-metrics-results/shannon-vector-group-significance.qzv

Observed Features

```
qiime diversity alpha-group-significance \
  --i-alpha-diversity g6-core-metrics-results/observed_features_vector.qza \
  --m-metadata-file "/Users/viviennelacy/Desktop/parent/gandfmeta.tsv" \
  --o-visualization g6-core-metrics-results/observed-features-group-significance.qzv
```

Output Visualization :

g6-core-metrics-results/observed-features-group-significance.qzv

Beta diversity in context of metadata

According to diet

```
qiime diversity beta-group-significance \
```

--i-distance-matrix g6-core-metrics-results/weighted_unifrac_distance_matrix.qza \

--m-metadata-file "/Users/viviennelacy/Desktop/parent/gandfmeta.tsv" \

--m-metadata-column diet \

--o-visualization g6-core-metrics-results/weighted-unifrac-diet-significance.qzv \

--p-pairwise

Output Visualization:

g6-core-metrics-results/weighted-unifrac-diet-significance.qzv

Taxonomic analysis

qiime taxa barplot \

--i-table G6-analysis-table.qza \

--i-taxonomy taxonomy.qza \

--m-metadata-file "/Users/viviennelacy/Desktop/parent/gandfmeta.tsv" \

--o-visualization g6-taxa-bar-plots.qzv

Output

g6-taxa-bar-plots.qzv

Differential Abundance Testing

qiime feature-table filter-samples \

```
  --i-table parent-table.qza \
  --m-metadata-file "/Users/viviennelacy/Desktop/parent/gandfmeta.tsv" \
  --p-where "[mod]='6'" \
  --o-filtered-table G6-table.qza
```

Output Artifact:

G6-table.qza

On the genus level

```
qiime taxa collapse \
  --i-table G6-table.qza \
  --i-taxonomy taxonomy.qza \
  --p-level 6 \
  --o-collapsed-table G6-table-level6.qza
```

Output Artifact:

G6-table-level6.qza

```
qiime composition add-pseudocount \
  --i-table G6-table-level6.qza \
  --o-composition-table comp-G6-table-level6-qza
```

Output Artifact:

comp-G6-table-level6-qza.qza

```
qiime composition ancom \
  --i-table comp-G6-table-level6-qza.qza \
  --m-metadata-file "/Users/viviennelacy/Desktop/parent/gandfmeta.tsv" \
  --m-metadata-column diet \
  --o-visualization level6-G6-ancom.qzv
```

Output Visualization:

level6-G6-ancom.qzv

At the species level

```
qiime taxa collapse \
  --i-table G6-table.qza \
  --i-taxonomy taxonomy.qza \
  --p-level 7 \
  --o-collapsed-table G6-table-level7.qza
```

Output Artifact:

G6-table-level7.qza

```
qiime composition add-pseudocount \
  --i-table G6-table-level7.qza \
  --o-composition-table comp-G6-table-level7-qza
```

Output Artifact:

comp-G6-table-level7-qza.qza

```
qiime composition ancom \
  --i-table comp-G6-table-level7-qza.qza \
  --m-metadata-file "/Users/viviennelacy/Desktop/parent/gandfmeta.tsv" \
  --m-metadata-column diet \
  --o-visualization level7-G6-ancom.qzv
```

Output Visualization:

Level7-G6-ancom.qzv

According to MD group at genus level

```
qiime feature-table filter-samples \
  --i-table parent-table.qza \
  --m-metadata-file "/Users/viviennelacy/Desktop/parent/gandfmeta.tsv" \
  --p-where "[diet]='MD'" \
  --o-filtered-table MD-table.qza
```

Output Artifact:

MD-table.qza

```
qiime taxa collapse \
  --i-table MD-table.qza \
  --i-taxonomy taxonomy.qza \
```

```
  --p-level 6 \
  --o-collapsed-table MD-table-level6.qza
```

Output Artifact:

MD-table-level6.qza

```
qiime composition add-pseudocount \
  --i-table MD-table-level6.qza \
  --o-composition-table comp-MD-table-level6
```

Output Artifact:

comp-MD-table-level6.qza

```
qiime composition ancom \
  --i-table comp-MD-table-level6.qza \
  --m-metadata-file "/Users/viviennelacy/Desktop/parent/gandfmeta.tsv" \
  --m-metadata-column mod \
  --o-visualization level6-MD-mod-ancom.qzv
```

Output Visualization:

level6-MD-mod-ancom.qzv

According to the TAD group at genus level

```
qiime feature-table filter-samples \
  --i-table parent-table.qza \
```

```
  --m-metadata-file "/Users/viviennelacy/Desktop/parent/gandfmeta.tsv" \
  --p-where "[diet]='TAD'" \
  --o-filtered-table TAD-table.qza
```

Output Artifact:

TAD-table.qza

```
qiime taxa collapse \
  --i-table TAD-table.qza \
  --i-taxonomy taxonomy.qza \
  --p-level 6 \
  --o-collapsed-table TAD-table-level6.qza
```

Output Artifact:

TAD-table-level6.qza

```
qiime composition add-pseudocount \
  --i-table TAD-table-level6.qza \
  --o-composition-table comp-TAD-table-level6
```

Output Artifact:

comp-TAD-table-level6.qza

```
qiime composition ancom \
  --i-table comp-TAD-table-level6.qza \
```

--m-metadata-file "/Users/viviennelacy/Desktop/parent/gandfmeta.tsv" \

--m-metadata-column mod \

--o-visualization level6-TAD-mod-ancom.qzv

Output Visualization:

level6-TAD-mod-ancom.qzv

G1: 0 MOD

Feature table of G1: 0 MOD

qiime feature-table filter-samples \

--i-table parent-table.qza \

--m-metadata-file "/Users/viviennelacy/Desktop/parent/gandfmeta.tsv" \

--p-where "[mod]='0'" \

--o-filtered-table G0-analysis-table.qza

Output Artifact:

G0-analysis-table.qza

Alpha and beta diversity core metrics

qiime diversity core-metrics-phylogenetic \

--i-phylogeny rooted-tree.qza \

```
  --i-table G0-analysis-table.qza \
  --p-sampling-depth 115 \
  --m-metadata-file "/Users/viviennelacy/Desktop/parent/gandfmeta.tsv" \
  --output-dir g0-core-metrics-results
```

Output Artifacts:

Saved FeatureTable[Frequency] to: gandf-core-metrics-results/rarefied_table.qza

Saved SampleData[AlphaDiversity] to: g0-core-metrics-results/faith_pd_vector.qza

Saved SampleData[AlphaDiversity] to: g0-core-metrics-results/observed_features_vector.qza

Saved SampleData[AlphaDiversity] to: g0-core-metrics-results/shannon_vector.qza

Saved SampleData[AlphaDiversity] to: g0-core-metrics-results/evenness_vector.qza

Saved DistanceMatrix to: g0-core-metrics-results/unweighted_unifrac_distance_matrix.qza

Saved DistanceMatrix to: g0-core-metrics-results/weighted_unifrac_distance_matrix.qza

Saved DistanceMatrix to: g0-core-metrics-results/jaccard_distance_matrix.qza

Saved DistanceMatrix to: g0-core-metrics-results/bray_curtis_distance_matrix.qza

Saved PCoAResults to: g0-core-metrics-results/unweighted_unifrac_pcoa_results.qza

Saved PCoAResults to: g0-core-metrics-results/weighted_unifrac_pcoa_results.qza

Saved PCoAResults to: g0-core-metrics-results/jaccard_pcoa_results.qza

Saved PCoAResults to: g0-core-metrics-results/bray_curtis_pcoa_results.qza

Output Visualizations:

Saved Visualization to: g0-core-metrics-results/unweighted_unifrac_emperor.qzv

Saved Visualization to: g0-core-metrics-results/weighted_unifrac_emperor.qzv

Saved Visualization to: g0-core-metrics-results/jaccard_emperor.qzv

Saved Visualization to: g0-core-metrics-results/bray_curtis_emperor.qzv

Alpha diversity in the context of metadata

Shannon index

```
qiime diversity alpha-group-significance \
  --i-alpha-diversity g0-core-metrics-results/shannon_vector.qza \
  --m-metadata-file "/Users/viviennelacy/Desktop/parent/gandfmeta.tsv" \
  --o-visualization g0-core-metrics-results/shannon-vector-group-significance.qzv
```

Output Visualization:

g0-core-metrics-results/shannon-vector-group-significance.qzv

Evenness

```
qiime diversity alpha-group-significance \
  --i-alpha-diversity g0-core-metrics-results/evenness_vector.qza \
  --m-metadata-file "/Users/viviennelacy/Desktop/parent/gandfmeta.tsv" \
  --o-visualization g0-core-metrics-results/evenness-group-significance.qzv
```

Output Visualization:

g0-core-metrics-results/evenness-group-significance.qzv

Observed features

```
qiime diversity alpha-group-significance \
  --i-alpha-diversity g0-core-metrics-results/observed_features_vector.qza \
  --m-metadata-file "/Users/viviennelacy/Desktop/parent/gandfmeta.tsv" \
  --o-visualization g0-core-metrics-results/observed-features-group-significance.qzv
```

Output Visualization:

g0-core-metrics-results/observed-features-group-significance.qzv

Beta diversity in the context of metadata

According to diet condition

```
qiime diversity beta-group-significance \
  --i-distance-matrix g0-core-metrics-results/weighted_unifrac_distance_matrix.qza \
 --m-metadata-file "/Users/viviennelacy/Desktop/d/QIIMEmeta.tsv" \
 --m-metadata-column diet \
 --o-visualization g0-core-metrics-results/unweighted-unifrac-diet-significance \
 --p-pairwise
```

Output Visualization:

g0-core-metrics-results/unweighted-unifrac-diet-significance

G1: 0 MOD v G1: 6 MOD

Feature table

```
qiime feature-table filter-samples \
  --i-table parent-table.qza \
  --m-metadata-file "/Users/viviennelacy/Desktop/parent/gandfmeta.tsv" \
  --p-where "[mod]='6' OR [mod]='0'" \
  --o-filtered-table G0andG6-analysis-table.qza
```

Output Artifact:

G0andG6-analysis-table.qza

Alpha and beta diversity metrics

```
qiime diversity core-metrics-phylogenetic \
  --i-phylogeny rooted-tree.qza \
  --i-table G0andG6-analysis-table.qza \
  --p-sampling-depth 115 \
  --m-metadata-file "/Users/viviennelacy/Desktop/parent/gandfmeta.tsv" \
  --output-dir g0andg6-core-metrics-results
```

Output Artifacts:

Saved FeatureTable[Frequency] to: g0andg6-core-metrics-results /rarefied_table.qza

Saved SampleData[AlphaDiversity] to: g0andg6-core-metrics-results/faith_pd_vector.qza

Saved SampleData[AlphaDiversity] to: g0andg6-core-metrics-results/observed_features_vector.qza

Saved SampleData[AlphaDiversity] to: g0andg6-core-metrics-results/shannon_vector.qza

Saved SampleData[AlphaDiversity] to: g0andg6-core-metrics-results/evenness_vector.qza

Saved DistanceMatrix to: g0andg6-core-metrics-results/unweighted_unifrac_distance_matrix.qza

Saved DistanceMatrix to: g0andg6-core-metrics-results/weighted_unifrac_distance_matrix.qza

Saved DistanceMatrix to: g0andg6-core-metrics-results/jaccard_distance_matrix.qza

Saved DistanceMatrix to: g0andg6-core-metrics-results/bray_curtis_distance_matrix.qza

Saved PCoAResults to: g0andg6-core-metrics-results/unweighted_unifrac_pcoa_results.qza

Saved PCoAResults to: g0andg6-core-metrics-results/weighted_unifrac_pcoa_results.qza

Saved PCoAResults to: g0andg6-core-metrics-results/jaccard_pcoa_results.qza

Saved PCoAResults to: g0andg6-core-metrics-results/bray_curtis_pcoa_results.qza

Output Visualizations:

Saved Visualization to: g0andg6-core-metrics-results/unweighted_unifrac_emperor.qzv

Saved Visualization to: g0andg6-core-metrics-results/weighted_unifrac_emperor.qzv

Saved Visualization to: g0andg6-core-metrics-results/jaccard_emperor.qzv

Saved Visualization to: g0andg6-core-metrics-results/bray_curtis_emperor.qzv

Alpha diversity in the context of metadata

Shannon index

```
qiime diversity alpha-group-significance \
  --i-alpha-diversity g0andg6-core-metrics-results /shannon_vector.qza \
  --m-metadata-file "/Users/viviennelacy/Desktop/parent/gandfmeta.tsv" \
  --o-visualization g0andg6-core-metrics-results /shannon-vector-group-significance.qzv
```

Output Visualization:

g0andg6-core-metrics-results /shannon-vector-group-significance.qzv

Evenness

```
qiime diversity alpha-group-significance \
  --i-alpha-diversity g0andg6-core-metrics-results /evenness_vector.qza \
  --m-metadata-file "/Users/viviennelacy/Desktop/parent/gandfmeta.tsv" \
  --o-visualization g0andg6-core-metrics-results /evenness-group-significance.qzv
```

Output Visualization:

g0andg6-core-metrics-results /evenness-group-significance.qzv

Observed features

```
qiime diversity alpha-group-significance \
  --i-alpha-diversity g0andg6-core-metrics-results /observed_features_vector.qza \
```

--m-metadata-file "/Users/viviennelacy/Desktop/parent/gandfmeta.tsv" \

--o-visualization g0andg6-core-metrics-results /observed-features-group-significance.qzv

Output Visualization:

g0andg6-core-metrics-results /observed-features-group-significance.qzv

Beta diversity in the context of metadata

According to month of age

qiime diversity beta-group-significance \

--i-distance-matrix g0andg6-core-metrics-results/weighted_unifrac_distance_matrix.qza \

--m-metadata-file "/Users/viviennelacy/Desktop/d/QIIMEmeta.tsv" \

--m-metadata-column genmod \

--o-visualization g0andg6-core-metrics-results/unweighted-unifrac-genmod-significance \

--p-pairwise

Output Visualization:

g0andg6-core-metrics-results/unweighted-unifrac-genmod-significance

F1 Analysis

New Feature Table

```
qiime feature-table filter-samples \
  --i-table table.qza \
  --m-metadata-file "/Users/viviennelacy/Desktop/doubid/QIIMEmeta.tsv" \
  --p-where "[mod]='0' AND [gen]='F' " \
  --o-filtered-table F0-analysis-table.qza
```

Output Artifact:

F0-analysis-table.qza

Alpha and beta diversity core metrics

```
qiime diversity core-metrics-phylogenetic \
  --i-phylogeny rooted-tree.qza \
  --i-table F0-analysis-table.qza \
  --p-sampling-depth 115 \
  --m-metadata-file  "/Users/viviennelacy/Desktop/doubid/QIIMEmeta.tsv" \
  --output-dir f0-core-metrics-results
```

Output Artifacts:

Saved FeatureTable[Frequency] to: g0andg6-core-metrics-results /rarefied_table.qza

Saved SampleData[AlphaDiversity] to: g0andg6-core-metrics-results/faith_pd_vector.qza

Saved SampleData[AlphaDiversity] to: g0andg6-core-metrics-results/observed_features_vector.qza

Saved SampleData[AlphaDiversity] to: g0andg6-core-metrics-results/shannon_vector.qza

Saved SampleData[AlphaDiversity] to: g0andg6-core-metrics-results/evenness_vector.qza

Saved DistanceMatrix to: g0andg6-core-metrics-results/unweighted_unifrac_distance_matrix.qza

Saved DistanceMatrix to: g0andg6-core-metrics-results/weighted_unifrac_distance_matrix.qza

Saved DistanceMatrix to: g0andg6-core-metrics-results/jaccard_distance_matrix.qza

Saved DistanceMatrix to: g0andg6-core-metrics-results/bray_curtis_distance_matrix.qza

Saved PCoAResults to: g0andg6-core-metrics-results/unweighted_unifrac_pcoa_results.qza

Saved PCoAResults to: g0andg6-core-metrics-results/weighted_unifrac_pcoa_results.qza

Saved PCoAResults to: g0andg6-core-metrics-results/jaccard_pcoa_results.qza

Saved PCoAResults to: g0andg6-core-metrics-results/bray_curtis_pcoa_results.qza

Output Visualizations:

Saved Visualization to: g0andg6-core-metrics-results/unweighted_unifrac_emperor.qzv

Saved Visualization to: g0andg6-core-metrics-results/weighted_unifrac_emperor.qzv

Saved Visualization to: g0andg6-core-metrics-results/jaccard_emperor.qzv

Saved Visualization to: g0andg6-core-metrics-results/bray_curtis_emperor.qzv

Alpha diversity in the context of metadata

Shannon Diversity

```
qiime diversity alpha-group-significance \
  --i-alpha-diversity f0-core-metrics-results/shannon_vector.qza \
  --m-metadata-file "/Users/viviennelacy/Desktop/doubid/QIIMEmeta.tsv" \
  --o-visualization f0-core-metrics-results/shannon-vector-group-significance.qzv
```

Output Visualization:

f0-core-metrics-results/shannon-vector-group-significance.qzv

Simpson's Evenness

```
qiime diversity alpha-group-significance \
  --i-alpha-diversity f0-core-metrics-results/evenness_vector.qza \
  --m-metadata-file "/Users/viviennelacy/Desktop/doubid/QIIMEmeta.tsv" \
  --o-visualization f0-core-metrics-results/evenness-group-significance.qzv
```

Output Visualization:

f0-core-metrics-results/evenness-group-significance.qzv

Observed Taxonomic Units

```
qiime diversity alpha-group-significance \
  --i-alpha-diversity f0-core-metrics-results/observed_features_vector.qza \
  --m-metadata-file "/Users/viviennelacy/Desktop/doubid/QIIMEmeta.tsv" \
  --o-visualization f0-core-metrics-results/observed-features-group-significance.qzv
```

Output Visualization:

f0-core-metrics-results/observed-features-group-significance.qzv

Beta diversity in the context of metadata

According to diet condition

```
qiime diversity beta-group-significance \
  --i-distance-matrix f0-core-metrics-results/weighted_unifrac_distance_matrix.qza\
 --m-metadata-file "/Users/viviennelacy/Desktop/FBandG6/G6FB.tsv" \
 --m-metadata-column diet \
 --o-visualization f0mdcore-unweighted-unifrac.qzv \
 --p-pairwise
```

Output Visualization

f0mdcore-unweighted-unifrac.qzv

F1: MD 0 MOD v G1: MD 6 MOD

New feature table

```
qiime feature-table filter-samples \
  --i-table table.qza \
  --m-metadata-file "/Users/viviennelacy/Desktop/FBandG6/G6FB.tsv" \
```

--p-where "[diet]='MD'" \

--o-filtered-table fbg6md-table.qza

Output Artifact:

fbg6md-table.qza

Alpha and beta diversity core metrics

qiime diversity core-metrics-phylogenetic \

--i-phylogeny rooted-tree.qza \

--i-table fbg6md-table.qza \

--p-sampling-depth 115 \

--m-metadata-file "/Users/viviennelacy/Desktop/FBandG6/G6FB.tsv" \

--output-dir f0andg6md-core-metrics-results

Output Artifacts:

Saved FeatureTable[Frequency] to: f0andg6md-core-metrics-results/rarefied_table.qza

Saved SampleData[AlphaDiversity] to: f0andg6md-core-metrics-results/faith_pd_vector.qza

Saved SampleData[AlphaDiversity] to: f0andg6md-core-metrics-results/observed_features_vector.qza

Saved SampleData[AlphaDiversity] to: f0andg6md-core-metrics-results/shannon_vector.qza

Saved SampleData[AlphaDiversity] to: f0andg6md-core-metrics-results/evenness_vector.qza

Saved DistanceMatrix to: f0andg6md-core-metrics-results/unweighted_unifrac_distance_matrix.qza

Saved DistanceMatrix to: f0andg6md-core-metrics-results/weighted_unifrac_distance_matrix.qza

Saved DistanceMatrix to: f0andg6md-core-metrics-results/jaccard_distance_matrix.qza

Saved DistanceMatrix to: f0andg6md-core-metrics-results/bray_curtis_distance_matrix.qza

Saved PCoAResults to: f0andg6md-core-metrics-results/unweighted_unifrac_pcoa_results.qza

Saved PCoAResults to: f0andg6md-core-metrics-results/weighted_unifrac_pcoa_results.qza

Saved PCoAResults to: f0andg6md-core-metrics-results/jaccard_pcoa_results.qza

Saved PCoAResults to: f0andg6md-core-metrics-results/bray_curtis_pcoa_results.qza

Output Visualizations:

Saved Visualization to: f0andg6md-core-metrics-results/unweighted_unifrac_emperor.qzv

Saved Visualization to: f0andg6md-core-metrics-results/weighted_unifrac_emperor.qzv

Saved Visualization to: f0andg6md-core-metrics-results/jaccard_emperor.qzv

Saved Visualization to: f0andg6md-core-metrics-results/bray_curtis_emperor.qzv

Alpha diversity in the context of metadata

Shannon Index

qiime diversity alpha-group-significance \

```
  --i-alpha-diversity f0andg6md-core-metrics-results/shannon_vector.qza \
  --m-metadata-file "/Users/viviennelacy/Desktop/FBandG6/G6FB.tsv" \
  --o-visualization f0andg6md-core-metrics-results/shannon_vector.qzv
```

Output Visualization:

f0andg6md-core-metrics-results/shannon_vector.qzv

Simpson's Evenness

```
qiime diversity alpha-group-significance \
  --i-alpha-diversity f0andg6md-core-metrics-results/evenness_vector.qza \
  --m-metadata-file "/Users/viviennelacy/Desktop/FBandG6/G6FB.tsv" \
  --o-visualization f0andg6md-evenness-group-significance.qzv
```

Output Visualization:

f0andg6md-evenness-group-significance.qzv

Observed Operational Taxonomic Units

```
qiime diversity alpha-group-significance \
  --i-alpha-diversity f0andg6md-core-metrics-results/observed-features-vector.qza \
  --m-metadata-file "/Users/viviennelacy/Desktop/FBandG6/G6FB.tsv" \
  --o-visualization f0andg6md-observed-features-vector.qzv
```

Output Visualization:

f0andg6md-observed-features-vector.qzv

Beta diversity in the context of metadata

According to generation (G1 vs F1)

```
qiime diversity beta-group-significance \
 --i-distance-matrix f0andg6md-core-metrics-results/weighted_unifrac_distance_matrix.qza\
 --m-metadata-file "/Users/viviennelacy/Desktop/FBandG6/G6FB.tsv" \
 --m-metadata-column gen \
 --o-visualization genfbg6mdcore-unweighted-unifrac.qzv \
 --p-pairwise
```

Output Visualization:

genfbg6mdcore-unweighted-unifrac.qzv

Taxa Bar Plots and Differential Abundance Testing

Differential abundance taxa barplots

```
qiime taxa barplot \
  --i-table fbg6md-table.qza \
  --i-taxonomy taxonomy.qza \
  --m-metadata-file "/Users/viviennelacy/Desktop/FBandG6/G6FB.tsv" \
  --o-visualization g6fbmd-taxa-bar-plots.qzv
```

Output Visualization:

g6fbmd-taxa-bar-plots.qzv

According to phylum level

```
qiime taxa collapse \
  --i-table fbg6md-table.qza \
  --i-taxonomy taxonomy.qza \
  --p-level 2 \
  --o-collapsed-table g6fbmd-table-level2.qza
```

Output Artifact:

g6fbmd-table-level2.qza

```
qiime composition add-pseudocount \
  --i-table g6fbmd-table-level2.qza \
  --o-composition-table comp-g6fbmd-table-level2
```

Output Artifact:

comp-g6fbmd-table-level2

```
qiime composition ancom \
  --i-table comp-g6fbmd-table-level2.qza \
  --m-metadata-file "/Users/viviennelacy/Desktop/FBandG6/G6FB.tsv" \
  --m-metadata-column gen \
```

```
  --o-visualization level2-g6fbmd-ancom.qzv
```

Output Visualization:

level2-g6fbmd-ancom.qzv

Taxa bar plots according to phylum level

```
qiime taxa barplot \
  --i-table fbg6md-table.qza \
  --i-taxonomy taxonomy.qza \
      --m-metadata-file "/Users/viviennelacy/Desktop/FBandG6/G6FB.tsv" \
  --o-visualization g6fbmd-taxa-bar-plots.qzv
```

Output Visualization:

g6fbmd-taxa-bar-plots.qzv

F1: TAD 0 MOD v G1: TAD 6 MOD

Feature Table

```
qiime feature-table filter-samples \
  --i-table table.qza \
  --m-metadata-file "/Users/viviennelacy/Desktop/FBandG6/G6FB.tsv" \
  --p-where "[diet]='TAD'" \
  --o-filtered-table fbg6tad-table.qza
```

Output Artifacts:

fbg6tad-table.qza

Alpha and beta diversity core metrics

```
qiime diversity core-metrics-phylogenetic \
  --i-phylogeny rooted-tree.qza \
  --i-table fbg6tad-table.qza \
  --p-sampling-depth 115 \
  --m-metadata-file "/Users/viviennelacy/Desktop/FBandG6/G6FB.tsv" \
  --output-dir f0andg6tad-core-metrics-results
```

Output Artifacts:

Saved FeatureTable[Frequency] to: f0andg6tad-core-metrics-results/rarefied_table.qza

Saved SampleData[AlphaDiversity] to: f0andg6tad-core-metrics-results/faith_pd_vector.qza

Saved SampleData[AlphaDiversity] to: f0andg6tad-core-metrics-results/observed_features_vector.qza

Saved SampleData[AlphaDiversity] to: f0andg6tad-core-metrics-results/shannon_vector.qza

Saved SampleData[AlphaDiversity] to: f0andg6tad-core-metrics-results/evenness_vector.qza

Saved DistanceMatrix to: f0andg6tad-core-metrics-results/unweighted_unifrac_distance_matrix.qza

Saved DistanceMatrix to: f0andg6tad-core-metrics-results/weighted_unifrac_distance_matrix.qza

Saved DistanceMatrix to: f0andg6tad-core-metrics-results/jaccard_distance_matrix.qza

Saved DistanceMatrix to: f0andg6tad-core-metrics-results/bray_curtis_distance_matrix.qza

Saved PCoAResults to: f0andg6tad-core-metrics-results/unweighted_unifrac_pcoa_results.qza

Saved PCoAResults to: f0andg6tad-core-metrics-results/weighted_unifrac_pcoa_results.qza

Saved PCoAResults to: f0andg6tad-core-metrics-results/jaccard_pcoa_results.qza

Saved PCoAResults to: f0andg6tad-core-metrics-results/bray_curtis_pcoa_results.qza

Output Visualizations:

Saved Visualization to: f0andg6tad-core-metrics-results/unweighted_unifrac_emperor.qzv

Saved Visualization to: f0andg6tad-core-metrics-results/weighted_unifrac_emperor.qzv

Saved Visualization to: f0andg6tad-core-metrics-results/jaccard_emperor.qzv

Saved Visualization to: f0andg6tad-core-metrics-results/bray_curtis_emperor.qzv

Alpha diversity in the context of metadata

Shannon Index

```
qiime diversity alpha-group-significance \
  --i-alpha-diversity f0andg6tad-core-metrics-results/shannon_vector.qza \
  --m-metadata-file "/Users/viviennelacy/Desktop/FBandG6/G6FB.tsv" \
```

--o-visualization f0andg6tad-core-metrics-results/shannon_vector.qzv

Output Visualizations:

f0andg6tad-core-metrics-results/shannon_vector.qzv

Simpson's Evenness

```
qiime diversity alpha-group-significance \
  --i-alpha-diversity f0andg6tad-core-metrics-results/evenness_vector.qza \
  --m-metadata-file "/Users/viviennelacy/Desktop/FBandG6/G6FB.tsv" \
  --o-visualization f0andg6tad-evenness-group-significance.qzv
```

Output Visualization:

f0andg6tad-evenness-group-significance.qzv

Observed Operational Taxonomic Units

```
qiime diversity alpha-group-significance \
  --i-alpha-diversity f0andg6tad-core-metrics-results/observed_features_vector.qza \
  --m-metadata-file "/Users/viviennelacy/Desktop/FBandG6/G6FB.tsv" \
  --o-visualization f0andg6tad-observed-features-vector.qzv
```

Output Visualization:

f0andg6tad-observed-features-vector.qzv

Beta diversity in the context of metadata

According to generation

```
qiime diversity beta-group-significance \
  --i-distance-matrix f0andg6tad-core-metrics-results/weighted_unifrac_distance_matrix.qza\
 --m-metadata-file "/Users/viviennelacy/Desktop/FBandG6/G6FB.tsv" \
 --m-metadata-column gen \
 --o-visualization genfbg6tadcore-unweighted-unifrac.qzv \
 --p-pairwise
```

Output Visualization:

genfbg6tadcore-unweighted-unifrac.qzv

Taxa bar plots

```
qiime taxa barplot \
  --i-table fbg6tad-table.qza \
  --i-taxonomy taxonomy.qza \
  --m-metadata-file "/Users/viviennelacy/Desktop/FBandG6/G6FB.tsv" \
  --o-visualization g6fbtad-taxa-bar-plots.qzv
```

Output Visualization

g6fbtad-taxa-bar-plots.qzv

Differential Abundance

At the phylum level

```
qiime taxa collapse \
  --i-table fbg6tad-table.qza \
  --i-taxonomy taxonomy.qza \
  --p-level 2 \
  --o-collapsed-table g6fbtad-table-level2.qza
```

Output Artifact:

g6fbtad-table-level2.qza

```
qiime composition add-pseudocount \
  --i-table g6fbtad-table-level2.qza \
  --o-composition-table comp-g6fbtad-table-level2
```

Output Artifact:

comp-g6fbtad-table-level2.qza

```
qiime composition ancom \
  --i-table comp-g6fbtad-table-level2.qza \
  --m-metadata-file "/Users/viviennelacy/Desktop/FBandG6/G6FB.tsv" \
  --m-metadata-column gen \
  --o-visualization level2-g6fbtad-ancom.qzv
```

Output Visualization:

level2-g6fbtad-ancom.qzv

Taxa bar plots

```
qiime taxa barplot \
 --i-table fbg6tad-table.qza \
 --i-taxonomy taxonomy.qza \
      --m-metadata-file "/Users/viviennelacy/Desktop/FBandG6/G6FB.tsv" \
 --o-visualization g6fbtad-taxa-bar-plots.qzv
```

Output Visualization:

g6fbtad-taxa-bar-plots.qzv

F1: 2 MOD

Feature Table

```
qiime feature-table filter-samples \
  --i-table table.qza \
  --m-metadata-file "/Users/viviennelacy/Desktop/doubid/g0f2.tsv" \
  --p-where "[mod]='2' AND [gen]='F' " \
  --o-filtered-table F2-analysis-table.qza
```

Output Artifact:

F2-analysis-table.qza

Alpha and beta diversity core metrics

```
qiime diversity core-metrics-phylogenetic \
  --i-phylogeny rooted-tree.qza \
  --i-table F2-analysis-table.qza \
  --p-sampling-depth 115 \
  --m-metadata-file "/Users/viviennelacy/Desktop/doubid/g0f2.tsv" \
  --output-dir f2-core-metrics-results
```

Output Artifacts:

Saved FeatureTable[Frequency] to: f2-core-metrics-results/rarefied_table.qza

Saved SampleData[AlphaDiversity] to: f2-core-metrics-results/faith_pd_vector.qza

Saved SampleData[AlphaDiversity] to: f2-core-metrics-results/observed_features_vector.qza

Saved SampleData[AlphaDiversity] to: f2-core-metrics-results/shannon_vector.qza

Saved SampleData[AlphaDiversity] to: f2-core-metrics-results/evenness_vector.qza

Saved DistanceMatrix to: f2-core-metrics-results/unweighted_unifrac_distance_matrix.qza

Saved DistanceMatrix to: f2-core-metrics-results/weighted_unifrac_distance_matrix.qza

Saved DistanceMatrix to: f2-core-metrics-results/jaccard_distance_matrix.qza

Saved DistanceMatrix to: f2-core-metrics-results/bray_curtis_distance_matrix.qza

Saved PCoAResults to: f2-core-metrics-results/unweighted_unifrac_pcoa_results.qza

Saved PCoAResults to: f2-core-metrics-results/weighted_unifrac_pcoa_results.qza

Saved PCoAResults to: f2-core-metrics-results/jaccard_pcoa_results.qza

Saved PCoAResults to: f2-core-metrics-results/bray_curtis_pcoa_results.qza

Output Visualizations:

Saved Visualization to: f2-core-metrics-results/unweighted_unifrac_emperor.qzv

Saved Visualization to: f2-core-metrics-results/weighted_unifrac_emperor.qzv

Saved Visualization to: f2-core-metrics-results/jaccard_emperor.qzv

Saved Visualization to: f2-core-metrics-results/bray_curtis_emperor.qzv

Alpha diversity in the context of metadata

Shannon index

```
qiime diversity alpha-group-significance \
  --i-alpha-diversity f2-core-metrics-results/shannon_vector.qza \
  --m-metadata-file "/Users/viviennelacy/Desktop/doubid/g0f2.tsv" \
  --o-visualization f2-core-metrics-results/shannon-vector-group-significance.qzv
```

Output Visualization:

f2-core-metrics-results/shannon-vector-group-significance.qzv

Simpson's Evenness

qiime diversity alpha-group-significance \

  --i-alpha-diversity f2-core-metrics-results/evenness_vector.qza \

  --m-metadata-file "/Users/viviennelacy/Desktop/doubid/g0f2.tsv" \

  --o-visualization f2-core-metrics-results/evenness-group-significance.qzv

Output Visualization:

f2-core-metrics-results/evenness-group-significance.qzv

Observed Operational Taxonomic Units

qiime diversity alpha-group-significance \

  --i-alpha-diversity f2-core-metrics-results/observed_features_vector.qza \

  --m-metadata-file "/Users/viviennelacy/Desktop/doubid/g0f2.tsv" \

  --o-visualization f2-core-metrics-results/observed-features-group-significance.qzv

Output Visualization:

f2-core-metrics-results/observed-features-group-significance.qzv

Beta diversity in the context of metadata

According to diet

qiime diversity beta-group-significance \

  --i-distance-matrix f2-core-metrics-results/weighted_unifrac_distance_matrix.qza\

 --m-metadata-file "/Users/viviennelacy/Desktop/doubid/g0f2.tsv" \

--m-metadata-column diet \

--o-visualization f2core-unweighted-unifrac.qzv \

--p-pairwise

Output Visualization:

f2core-unweighted-unifrac.qzv

F1: 2 MOD v G1: 0 MOD

Feature Table

qiime feature-table filter-samples \

  --i-table table.qza \

  --m-metadata-file "/Users/viviennelacy/Desktop/doubid/g0f2.tsv" \

  --o-filtered-table F2GB-analysis-table.qza

Output Artifact:

F2GB-analysis-table.qza

Alpha and beta diversity core metrics

qiime diversity core-metrics-phylogenetic \

  --i-phylogeny rooted-tree.qza \

  --i-table F2GB-analysis-table.qza \

```
  --p-sampling-depth 115 \
  --m-metadata-file  "/Users/viviennelacy/Desktop/doubid/g0f2.tsv" \
  --output-dir f2gb-core-metrics-results
```

Output Artifacts:

```
Saved FeatureTable[Frequency] to: f2gb-core-metrics-results/rarefied_table.qza
Saved SampleData[AlphaDiversity] to: f2gb-core-metrics-results/faith_pd_vector.qza
Saved SampleData[AlphaDiversity] to: f2gb-core-metrics-results/observed_features_vector.qza
Saved SampleData[AlphaDiversity] to: f2gb-core-metrics-results/shannon_vector.qza
Saved SampleData[AlphaDiversity] to: f2gb-core-metrics-results/evenness_vector.qza
Saved DistanceMatrix to: f2gb-core-metrics-results/unweighted_unifrac_distance_matrix.qza
Saved DistanceMatrix to: f2gb-core-metrics-results/weighted_unifrac_distance_matrix.qza
Saved DistanceMatrix to: f2gb-core-metrics-results/jaccard_distance_matrix.qza
Saved DistanceMatrix to: f2gb-core-metrics-results/bray_curtis_distance_matrix.qza
Saved PCoAResults to: f2gb-core-metrics-results/unweighted_unifrac_pcoa_results.qza
Saved PCoAResults to: f2gb-core-metrics-results/weighted_unifrac_pcoa_results.qza
Saved PCoAResults to: f2gb-core-metrics-results/jaccard_pcoa_results.qza
Saved PCoAResults to: f2gb-core-metrics-results/bray_curtis_pcoa_results.qza
```

Output Visualizations:

```
Saved Visualization to: f2gb-core-metrics-results/unweighted_unifrac_emperor.qzv
```

Saved Visualization to: f2gb-core-metrics-results/weighted_unifrac_emperor.qzv

Saved Visualization to: f2gb-core-metrics-results/jaccard_emperor.qzv

Saved Visualization to: f2gb-core-metrics-results/bray_curtis_emperor.qzv

Alpha diversity in the context of metadata

Shannon index

```
qiime diversity alpha-group-significance \
  --i-alpha-diversity f2gb-core-metrics-results/shannon_vector.qza \
  --m-metadata-file "/Users/viviennelacy/Desktop/doubid/g0f2.tsv" \
  --o-visualization f2gb-core-metrics-results/shannon-vector-group-significance.qzv
```

Output Visualization:

f2gb-core-metrics-results/shannon-vector-group-significance.qzv

Simpson's Evenness

```
qiime diversity alpha-group-significance \
  --i-alpha-diversity f2gb-core-metrics-results/evenness_vector.qza \
  --m-metadata-file "/Users/viviennelacy/Desktop/doubid/g0f2.tsv" \
  --o-visualization f2gb-core-metrics-results/evenness-group-significance.qzv
```

Output Visualization:

f2gb-core-metrics-results/evenness-group-significance.qzv

Observed Operational Taxonomic Unit

```
qiime diversity alpha-group-significance \
  --i-alpha-diversity f2gb-core-metrics-results/observed_features_vector.qza \
  --m-metadata-file "/Users/viviennelacy/Desktop/doubid/g0f2.tsv" \
  --o-visualization f2gb-core-metrics-results/observed-features-group-significance.qzv
```

Output Visualization:

f2gb-core-metrics-results/observed-features-group-significance.qzv

Beta diversity in the context of metadata

According to generation

```
qiime diversity beta-group-significance \
  --i-distance-matrix f2gb-core-metrics-results/weighted_unifrac_distance_matrix.qza\
 --m-metadata-file "/Users/viviennelacy/Desktop/doubid/g0f2.tsv" \
 --m-metadata-column gen \
 --o-visualization f2gbcore-unweighted-unifrac.qzv \
 --p-pairwise
```

Output Visualization:

f2gbcore-unweighted-unifrac.qzv

Taxa bar plot

```
qiime taxa barplot \
 --i-table F2GB-analysis-table.qza \
 --i-taxonomy taxonomy.qza \
      --m-metadata-file "/Users/viviennelacy/Desktop/doubid/g0f2.tsv" \
 --o-visualization f2gb-taxa-bar-plots.qzv
```

Output Visualization:

f2gb-taxa-bar-plots.qzv

Differential abundance

At phylum level

```
qiime taxa collapse \
  --i-table F2GB-analysis-table.qza \
  --i-taxonomy taxonomy.qza \
  --p-level 2 \
  --o-collapsed-table f2gb-table-level2.qza
```

Output Artifact:

f2gb-table-level2.qza

```
qiime composition add-pseudocount \
```

```
  --i-table f2gb-table-level2.qza \
  --o-composition-table comp-f2gb-table-level2
qiime composition ancom \
  --i-table comp-f2gb-table-level2.qza \
  --m-metadata-file "/Users/viviennelacy/Desktop/doubid/g0f2.tsv" \
  --m-metadata-column gen \
  --o-visualization level2-f2gbtad-ancom.qzv
```

Output Visualization:

level2-f2gbtad-ancom.qzv

Taxa bar plots

```
qiime taxa barplot \
 --i-table F2GB-analysis-table.qza \
 --i-taxonomy taxonomy.qza \
      --m-metadata-file "/Users/viviennelacy/Desktop/doubid/g0f2.tsv" \
 --o-visualization g0f2tad-taxa-bar-plots.qzv
```

Output Visualization:

g0f2tad-taxa-bar-plots.qzv

Appendix D:

Experimental Diet Ingredients (Braden-Khule, 2024).

Ingredients (grams)	**Mediterranean Diet**	**Western Diet**
Protein Sources		
Casein	0	165.5
Soy Protein	47	0
Fish Protein	47	0
Egg White	47	0
DL-methionine	1.9	0.3
L-Cystine	3	3
Carbohydrate Sources		
Corn Starch	0	370.5
Brown Rice Flour	205	0
Wheat Starch	205	0
Maltodextrin 10	125	125
Dextrose	0	0
Fiber Sources		
Cellulose, BW200	50	50
Psyllium	50	0
Inulin	50	0

Fat Sources		
Soybean Oil	0	0
Corn Oil	0	0
Safflower Oil	0	12
Beef Fat, Bunge	3	106.3
Butter, Anhydrous	16	34
Flaxseed Oil	7	0
Menhaden Oil, ARBP-F	10	0
Olive Oil	107	0
Other Micronutrients		
Mineral Mix S10026	10	10
DiCalcium Phosphate	13	13
Calcium Carbonate	5.5	5.5
Potassium Citrate, 1 H2O	16.5	16.5
Vitamin Mix V10001	10	10
Biotin (1%)	0.1	0
Choline Chloride	3	1.07
Total	**1032.0000 gms**	**922.672 gms**

Experimental Diet Macro ingredients (Braden-Khule, 2024).

Macronutrients	**Mediterranean Diet**	**Western Diet**

Macronutrients (grams)		
Protein (gms)	147.2	147.3
Carbohydrate (gms)	495.3	495.5
Fat (gms)	153.2	153.1
Fiber (gms)	153.7	50.0
Macronutrients g%		
Protein	14.3	16.0
Carbohydrate	48.0	53.7
Fat	14.8	16.6
Fiber	14.9	5.4
Macronutrients kcal		
Protein	*589*	*589*
Carbohydrate	*1981*	*1982*
Fat	*1379*	*1378*
Total kcal	***3949***	***3949***
Macronutrients kcal%		
Protein	*15*	*15*
Carbohydrate	*50*	*50*
Fat	*35*	*35*

Fats (grams)		
Saturated Fatty Acids	29.5	74.4
Monounsaturated Fatty Acids	86.2	54.0
Polyunsaturated Fatty Acids	24.4	14.1
n-6	15.9	13.4
n-3	8.0	0.9
n-6/n-3 Ratio	2.0	15.6
Fats kcal%		
Saturated Fatty Acids	6.7	17.0
Monounsaturated Fatty Acids	19.6	12.3
Polyunsaturated Fatty Acids	5.6	3.2

BIBLIOGRAPHY

Abuznait, A. H., Qosa, H., Busnena, B. A., El Sayed, K. A., & Kaddoumi, A. (2013). Olive-oil-derived oleocanthal enhances beta-amyloid clearance as a potential neuroprotective mechanism against Alzheimer's disease: in vitro and in vivo studies. *ACS Chem Neurosci*, *4*(6), 973-982. https://doi.org/10.1021/cn400024q

Agus, A., Denizot, J., Thevenot, J., Martinez-Medina, M., Massier, S., Sauvanet, P., Bernalier-Donadille, A., Denis, S., Hofman, P., Bonnet, R., Billard, E., & Barnich, N. (2016). Western diet induces a shift in microbiota composition enhancing susceptibility to Adherent-Invasive E. coli infection and intestinal inflammation. *Sci Rep*, *6*, 19032. https://doi.org/10.1038/srep19032

Alzheimer's Association 2023 Annual Report. (2023).

Andreu-Reinon, M. E., Chirlaque, M. D., Gavrila, D., Amiano, P., Mar, J., Tainta, M., Ardanaz, E., Larumbe, R., Colorado-Yohar, S. M., Navarro-Mateu, F., Navarro, C., & Huerta, J. M. (2021). Mediterranean Diet and Risk of Dementia and Alzheimer's Disease in the EPIC-Spain Dementia Cohort Study. *Nutrients*, *13*(2). https://doi.org/10.3390/nu13020700

Araujo, G. R. L., Marques, H. S., Santos, M. L. C., da Silva, F. A. F., da Brito, B. B., Correa Santos, G. L., & de Melo, F. F. (2022). Helicobacter pylori infection: How does age influence the inflammatory pattern? *World J Gastroenterol*, *28*(4), 402-411. https://doi.org/10.3748/wjg.v28.i4.402

Aridi, Y. S., Walker, J. L., & Wright, O. R. L. (2017). The Association between the Mediterranean Dietary Pattern and Cognitive Health: A Systematic Review. *Nutrients*, *9*(7). https://doi.org/10.3390/nu9070674

Backhed, F., Roswall, J., Peng, Y., Feng, Q., Jia, H., Kovatcheva-Datchary, P., Li, Y., Xia, Y., Xie, H., Zhong, H., Khan, M. T., Zhang, J., Li, J., Xiao, L., Al-Aama, J., Zhang, D., Lee,

Y. S., Kotowska, D., Colding, C., . . . Wang, J. (2015). Dynamics and Stabilization of the Human Gut Microbiome during the First Year of Life. *Cell Host Microbe*, *17*(6), 852. https://doi.org/10.1016/j.chom.2015.05.012

Beam, A., Clinger, E., & Hao, L. (2021). Effect of Diet and Dietary Components on the Composition of the Gut Microbiota. *Nutrients*, *13*(8). https://doi.org/10.3390/nu13082795

Bello, S., McQuay, S., Rudra, B., & Gupta, R. S. (2024). Robust demarcation of the family Peptostreptococcaceae and its main genera based on phylogenomic studies and taxon-specific molecular markers. *Int J Syst Evol Microbiol*, *74*(2). https://doi.org/10.1099/ijsem.0.006247

Bokulich, N. A., Kaehler, B. D., Rideout, J. R., Dillon, M., Bolyen, E., Knight, R., Huttley, G. A., & Gregory Caporaso, J. (2018). Optimizing taxonomic classification of marker-gene amplicon sequences with QIIME 2's q2-feature-classifier plugin. *Microbiome*, *6*(1), 90. https://doi.org/10.1186/s40168-018-0470-z

Bolyen, E., Rideout, J. R., Dillon, M. R., Bokulich, N. A., Abnet, C. C., Al-Ghalith, G. A., Alexander, H., Alm, E. J., Arumugam, M., Asnicar, F., Bai, Y., Bisanz, J. E., Bittinger, K., Brejnrod, A., Brislawn, C. J., Brown, C. T., Callahan, B. J., Caraballo-Rodriguez, A. M., Chase, J., . . . Caporaso, J. G. (2019). Reproducible, interactive, scalable and extensible microbiome data science using QIIME 2. *Nat Biotechnol*, *37*(8), 852-857. https://doi.org/10.1038/s41587-019-0209-9

Borra, M. T., Smith, B. C., & Denu, J. M. (2005). Mechanism of human SIRT1 activation by resveratrol. *J Biol Chem*, *280*(17), 17187-17195. https://doi.org/10.1074/jbc.M501250200

Braden-Khule, P. N., Lacy, V. A., Brice, K. N., Bertrand, M. E., Uras, H. B., Shoffner, C., Fischer, B. E., Rana, A., Willis, J. L., Boehm, G. W., Chumley, M. J. (2024). *Food for*

Thought: A Comprehensive Mediterranean Diet Protects Against Cognitive and Behavioral Deficits, Adiposity, and Alzhiemer's Disease-Related Markers, Compared to a Macronutrient-Matched Typical American Diet.

Bruce-Keller, A. J., Salbaum, J. M., Luo, M., Blanchard, E. t., Taylor, C. M., Welsh, D. A., & Berthoud, H. R. (2015). Obese-type gut microbiota induce neurobehavioral changes in the absence of obesity. *Biol Psychiatry*, *77*(7), 607-615. https://doi.org/10.1016/j.biopsych.2014.07.012

Callahan, B. J., McMurdie, P. J., Rosen, M. J., Han, A. W., Johnson, A. J., & Holmes, S. P. (2016). DADA2: High-resolution sample inference from Illumina amplicon data. *Nat Methods*, *13*(7), 581-583. https://doi.org/10.1038/nmeth.3869

Chen, G. F., Xu, T. H., Yan, Y., Zhou, Y. R., Jiang, Y., Melcher, K., & Xu, H. E. (2017). Amyloid beta: structure, biology and structure-based therapeutic development. *Acta Pharmacol Sin*, *38*(9), 1205-1235. https://doi.org/10.1038/aps.2017.28

Christ, A., Lauterbach, M., & Latz, E. (2019). Western Diet and the Immune System: An Inflammatory Connection. *Immunity*, *51*(5), 794-811. https://doi.org/10.1016/j.immuni.2019.09.020

De-Paula, V. J., Radanovic, M., Diniz, B. S., & Forlenza, O. V. (2012). Alzheimer's disease. *Subcell Biochem*, *65*, 329-352. https://doi.org/10.1007/978-94-007-5416-4_14

den Besten, G., van Eunen, K., Groen, A. K., Venema, K., Reijngoud, D. J., & Bakker, B. M. (2013). The role of short-chain fatty acids in the interplay between diet, gut microbiota, and host energy metabolism. *J Lipid Res*, *54*(9), 2325-2340. https://doi.org/10.1194/jlr.R036012

Drummond, E., Pires, G., MacMurray, C., Askenazi, M., Nayak, S., Bourdon, M., Safar, J., Ueberheide, B., & Wisniewski, T. (2020). Phosphorylated tau interactome in the human

Alzheimer's disease brain. *Brain*, *143*(9), 2803-2817. https://doi.org/10.1093/brain/awaa223

El Aidy, S., Hooiveld, G., Tremaroli, V., Backhed, F., & Kleerebezem, M. (2013). The gut microbiota and mucosal homeostasis: colonized at birth or at adulthood, does it matter? *Gut Microbes*, *4*(2), 118-124. https://doi.org/10.4161/gmic.23362

Garcia-Montero, C., Fraile-Martinez, O., Gomez-Lahoz, A. M., Pekarek, L., Castellanos, A. J., Noguerales-Fraguas, F., Coca, S., Guijarro, L. G., Garcia-Honduvilla, N., Asunsolo, A., Sanchez-Trujillo, L., Lahera, G., Bujan, J., Monserrat, J., Alvarez-Mon, M., Alvarez-Mon, M. A., & Ortega, M. A. (2021). Nutritional Components in Western Diet Versus Mediterranean Diet at the Gut Microbiota-Immune System Interplay. Implications for Health and Disease. *Nutrients*, *13*(2). https://doi.org/10.3390/nu13020699

Haskey, N., Ye, J., Estaki, M., Verdugo Meza, A. A., Barnett, J. A., Yousefi, M., Birnie, B. W., Gruenheid, S., Ghosh, S., & Gibson, D. L. (2022). A Mediterranean-like fat blend protects against the development of severe colitis in the mucin-2 deficient murine model. *Gut Microbes*, *14*(1), 2055441. https://doi.org/10.1080/19490976.2022.2055441

Heravi, F. S., Naseri, K., & Hu, H. (2023). Gut Microbiota Composition in Patients with Neurodegenerative Disorders (Parkinson's and Alzheimer's) and Healthy Controls: A Systematic Review. *Nutrients*, *15*(20). https://doi.org/10.3390/nu15204365

Hevia, A., Delgado, S., Sanchez, B., & Margolles, A. (2015). Molecular Players Involved in the Interaction Between Beneficial Bacteria and the Immune System. *Front Microbiol*, *6*, 1285. https://doi.org/10.3389/fmicb.2015.01285

Julien, C., Tremblay, C., Phivilay, A., Berthiaume, L., Emond, V., Julien, P., & Calon, F. (2010). High-fat diet aggravates amyloid-beta and tau pathologies in the 3xTg-AD mouse model. *Neurobiol Aging*, *31*(9), 1516-1531. https://doi.org/10.1016/j.neurobiolaging.2008.08.022

Kesika, P., Suganthy, N., Sivamaruthi, B. S., & Chaiyasut, C. (2021). Role of gut-brain axis, gut microbial composition, and probiotic intervention in Alzheimer's disease. *Life Sci*, *264*, 118627. https://doi.org/10.1016/j.lfs.2020.118627

Lupp, C., Robertson, M. L., Wickham, M. E., Sekirov, I., Champion, O. L., Gaynor, E. C., & Finlay, B. B. (2007). Host-mediated inflammation disrupts the intestinal microbiota and promotes the overgrowth of Enterobacteriaceae. *Cell Host Microbe*, *2*(2), 119-129. https://doi.org/10.1016/j.chom.2007.06.010

Lyte, M. (2011). Probiotics function mechanistically as delivery vehicles for neuroactive compounds: Microbial endocrinology in the design and use of probiotics. *Bioessays*, *33*(8), 574-581. https://doi.org/10.1002/bies.201100024

Mackie, R. I., Sghir, A., & Gaskins, H. R. (1999). Developmental microbial ecology of the neonatal gastrointestinal tract. *Am J Clin Nutr*, *69*(5), 1035S-1045S. https://doi.org/10.1093/ajcn/69.5.1035s

Malesza, I. J., Malesza, M., Walkowiak, J., Mussin, N., Walkowiak, D., Aringazina, R., Bartkowiak-Wieczorek, J., & Madry, E. (2021). High-Fat, Western-Style Diet, Systemic Inflammation, and Gut Microbiota: A Narrative Review. *Cells*, *10*(11). https://doi.org/10.3390/cells10113164

Mancilla, V. J., Braden-Kuhle, P. N., Brice, K. N., Mann, A. E., Williams, M. T., Zhang, Y., Chumley, M. J., Barber, R. C., White, S. N., Boehm, G. W., & Allen, M. S. (2023). A Synthetic Formula Amino Acid Diet Leads to Microbiome Dysbiosis, Reduced Colon Length, Inflammation, and Altered Locomotor Activity in C57BL/6J Mice. *Microorganisms*, *11*(11). https://doi.org/10.3390/microorganisms11112694

Mendez, M. F. (2019). Early-onset Alzheimer Disease and Its Variants. *Continuum (Minneap Minn)*, *25*(1), 34-51. https://doi.org/10.1212/CON.0000000000000687

Meropol, S. B., & Edwards, A. (2015). Development of the infant intestinal microbiome: A bird's eye view of a complex process. *Birth Defects Res C Embryo Today*, *105*(4), 228-239. https://doi.org/10.1002/bdrc.21114

Montenegro, J., Armet, A. M., Willing, B. P., Deehan, E. C., Fassini, P. G., Mota, J. F., Walter, J., & Prado, C. M. (2023). Exploring the Influence of Gut Microbiome on Energy Metabolism in Humans. *Adv Nutr*, *14*(4), 840-857. https://doi.org/10.1016/j.advnut.2023.03.015

Mtaweh, H., Tuira, L., Floh, A. A., & Parshuram, C. S. (2018). Indirect Calorimetry: History, Technology, and Application. *Front Pediatr*, *6*, 257. https://doi.org/10.3389/fped.2018.00257

Murray, E. R., Kemp, M., & Nguyen, T. T. (2022). The Microbiota-Gut-Brain Axis in Alzheimer's Disease: A Review of Taxonomic Alterations and Potential Avenues for Interventions. *Arch Clin Neuropsychol*, *37*(3), 595-607. https://doi.org/10.1093/arclin/acac008

Naseri, N. N., Wang, H., Guo, J., Sharma, M., & Luo, W. (2019). The complexity of tau in Alzheimer's disease. *Neurosci Lett*, *705*, 183-194. https://doi.org/10.1016/j.neulet.2019.04.022

Ott, B., Skurk, T., Lagkouvardos, L., Fischer, S., Buttner, J., Lichtenegger, M., Clavel, T., Lechner, A., Rychlik, M., Haller, D., & Hauner, H. (2018). Short-Term Overfeeding with Dairy Cream Does Not Modify Gut Permeability, the Fecal Microbiota, or Glucose Metabolism in Young Healthy Men. *J Nutr*, *148*(1), 77-85. https://doi.org/10.1093/jn/nxx020

Pistell, P. J., Morrison, C. D., Gupta, S., Knight, A. G., Keller, J. N., Ingram, D. K., & Bruce-Keller, A. J. (2010). Cognitive impairment following high fat diet consumption is

associated with brain inflammation. *J Neuroimmunol*, *219*(1-2), 25-32. https://doi.org/10.1016/j.jneuroim.2009.11.010

Pluta, R., Ulamek-Koziol, M., Januszewski, S., & Czuczwar, S. J. (2020). Gut microbiota and pro/prebiotics in Alzheimer's disease. *Aging (Albany NY)*, *12*(6), 5539-5550. https://doi.org/10.18632/aging.102930

Primec, M., Micetic-Turk, D., & Langerholc, T. (2017). Analysis of short-chain fatty acids in human feces: A scoping review. *Anal Biochem*, *526*, 9-21. https://doi.org/10.1016/j.ab.2017.03.007

Purnell, J. Q. (2023). What is Obesity?: Definition as a Disease, with Implications for Care. *Gastroenterol Clin North Am*, *52*(2), 261-275. https://doi.org/10.1016/j.gtc.2023.03.001

Rakhra, V., Galappaththy, S. L., Bulchandani, S., & Cabandugama, P. K. (2020). Obesity and the Western Diet: How We Got Here. *Mo Med*, *117*(6), 536-538. https://www.ncbi.nlm.nih.gov/pubmed/33311784

Rastogi, S., & Singh, A. (2022). Gut microbiome and human health: Exploring how the probiotic genus Lactobacillus modulate immune responses. *Front Pharmacol*, *13*, 1042189. https://doi.org/10.3389/fphar.2022.1042189

Ringel-Kulka, T., Cheng, J., Ringel, Y., Salojarvi, J., Carroll, I., Palva, A., de Vos, W. M., & Satokari, R. (2013). Intestinal microbiota in healthy U.S. young children and adults--a high throughput microarray analysis. *PLoS One*, *8*(5), e64315. https://doi.org/10.1371/journal.pone.0064315

Safaei, M., Sundararajan, E. A., Driss, M., Boulila, W., & Shapi'i, A. (2021). A systematic literature review on obesity: Understanding the causes & consequences of obesity and reviewing various machine learning approaches used to predict obesity. *Comput Biol Med*, *136*, 104754. https://doi.org/10.1016/j.compbiomed.2021.104754

Sanchez-Delgado, G., & Ravussin, E. (2020). Assessment of energy expenditure: are calories measured differently for different diets? *Curr Opin Clin Nutr Metab Care*, *23*(5), 312-318. https://doi.org/10.1097/MCO.0000000000000680

Singh, R. K., Chang, H. W., Yan, D., Lee, K. M., Ucmak, D., Wong, K., Abrouk, M., Farahnik, B., Nakamura, M., Zhu, T. H., Bhutani, T., & Liao, W. (2017). Influence of diet on the gut microbiome and implications for human health. *J Transl Med*, *15*(1), 73. https://doi.org/10.1186/s12967-017-1175-y

Spor, A., Koren, O., & Ley, R. (2011). Unravelling the effects of the environment and host genotype on the gut microbiome. *Nat Rev Microbiol*, *9*(4), 279-290. https://doi.org/10.1038/nrmicro2540

Statovci, D., Aguilera, M., MacSharry, J., & Melgar, S. (2017). The Impact of Western Diet and Nutrients on the Microbiota and Immune Response at Mucosal Interfaces. *Front Immunol*, *8*, 838. https://doi.org/10.3389/fimmu.2017.00838

Stecher, B., Robbiani, R., Walker, A. W., Westendorf, A. M., Barthel, M., Kremer, M., Chaffron, S., Macpherson, A. J., Buer, J., Parkhill, J., Dougan, G., von Mering, C., & Hardt, W. D. (2007). Salmonella enterica serovar typhimurium exploits inflammation to compete with the intestinal microbiota. *PLoS Biol*, *5*(10), 2177-2189. https://doi.org/10.1371/journal.pbio.0050244

Stefaniak, O., Dobrzynska, M., Drzymala-Czyz, S., & Przyslawski, J. (2022). Diet in the Prevention of Alzheimer's Disease: Current Knowledge and Future Research Requirements. *Nutrients*, *14*(21). https://doi.org/10.3390/nu14214564

Stierman, B. A., J; Carrol, M; Chen, T; Davy, O; Fink, S; Fryar, C; Gu, Q; Hales, C; Hughes, J; Ostchega, Y; Stoarndt, R; Akinbami, L. (2021). *National Health and Nutrition Examination Survey 2017-March 2020 Prepandemic Data Files - Development of Files*

and Prevalent Estimates for Selected Health Outcomes (National Health Statistics Report, Issue.

Trichopoulou, A., Kyrozis, A., Rossi, M., Katsoulis, M., Trichopoulos, D., La Vecchia, C., & Lagiou, P. (2015). Mediterranean diet and cognitive decline over time in an elderly Mediterranean population. *Eur J Nutr*, *54*(8), 1311-1321. https://doi.org/10.1007/s00394-014-0811-z

Trichopoulou, A., Martinez-Gonzalez, M. A., Tong, T. Y., Forouhi, N. G., Khandelwal, S., Prabhakaran, D., Mozaffarian, D., & de Lorgeril, M. (2014). Definitions and potential health benefits of the Mediterranean diet: views from experts around the world. *BMC Med*, *12*, 112. https://doi.org/10.1186/1741-7015-12-112

Troci, A., Philippen, S., Rausch, P., Rave, J., Weyland, G., Niemann, K., Jessen, K., Schmill, L. P., Aludin, S., Franke, A., Berg, D., Bang, C., & Bartsch, T. (2024). Disease- and stage-specific alterations of the oral and fecal microbiota in Alzheimer's disease. *PNAS Nexus*, *3*(1), pgad427. https://doi.org/10.1093/pnasnexus/pgad427

Vogt, N. M., Kerby, R. L., Dill-McFarland, K. A., Harding, S. J., Merluzzi, A. P., Johnson, S. C., Carlsson, C. M., Asthana, S., Zetterberg, H., Blennow, K., Bendlin, B. B., & Rey, F. E. (2017). Gut microbiome alterations in Alzheimer's disease. *Sci Rep*, *7*(1), 13537. https://doi.org/10.1038/s41598-017-13601-y

Westerterp, K. R. (2017). Doubly labelled water assessment of energy expenditure: principle, practice, and promise. *Eur J Appl Physiol*, *117*(7), 1277-1285. https://doi.org/10.1007/s00421-017-3641-x

Wieckowska-Gacek, A., Mietelska-Porowska, A., Wydrych, M., & Wojda, U. (2021). Western diet as a trigger of Alzheimer's disease: From metabolic syndrome and systemic

inflammation to neuroinflammation and neurodegeneration. *Ageing Res Rev*, *70*, 101397. https://doi.org/10.1016/j.arr.2021.101397

Wu, H., Zhang, W., Huang, M., Lin, X., & Chiou, J. (2023). Prolonged High-Fat Diet Consumption throughout Adulthood in Mice Induced Neurobehavioral Deterioration via Gut-Brain Axis. *Nutrients*, *15*(2). https://doi.org/10.3390/nu15020392

Wu, L., Han, Y., Zheng, Z., Zhu, S., Chen, J., Yao, Y., Yue, S., Teufel, A., Weng, H., Li, L., & Wang, B. (2021). Obeticholic Acid Inhibits Anxiety via Alleviating Gut Microbiota-Mediated Microglia Accumulation in the Brain of High-Fat High-Sugar Diet Mice. *Nutrients*, *13*(3). https://doi.org/10.3390/nu13030940

Zhao, F., Song, S., Ma, Y., Xu, X., Zhou, G., & Li, C. (2019). A Short-Term Feeding of Dietary Casein Increases Abundance of Lactococcus lactis and Upregulates Gene Expression Involving Obesity Prevention in Cecum of Young Rats Compared With Dietary Chicken Protein. *Front Microbiol*, *10*, 2411. https://doi.org/10.3389/fmicb.2019.02411

VITA

PERSONAL BACKGROUND

Vivienne Ann-Marie Lacy

Highlands Ranch, Colorado

Daughter of Martine Lacy and Terrance Lacy

EDUCATION

Diploma, Rock Canyon High School, Highlands Ranch, Colorado, 2019

Bachelor of Science, Microbiology, Texas Tech University, Lubbock, Texas, 2022

Master of Science, Biology, Texas Christian University, 2024

EXPERIENCE

Research Assistant, Department of Biology, Texas Tech University, 2020-2022

Natural Science Research Lab Assistant, Texas Tech University, 2021-2022

Teaching Assistantship, Texas Chrisitan University, 2022-present

PROFESSIONAL MEMBERSHIP

Academic Society for Functional Foods and Bioactive Compounds, 2020-2021

American Society of Mammologists, 2021-2022

Society for Neuroscience, 2022-2023

ABSTRACT

COMPARING THE EFFECTS OF A COMPREHENSIVE TYPICAL AMERICAN DIET OR MEDITERRANEAN DIET ON GUT MICROBIOME COMPOSITION

By Vivienne Lacy

Department of Biology

Texas Christian University

Thesis Advisor: Michael Chumley, Professor of Biology

Alzheimer's disease (AD) is a neurodegenerative disease with several factors implicated in its progression, including the chronic consumption of a Western diet. Current diet literature utilizes models that are not translational to what a typical American would consume. Therefore, a previous study from our team explored the effect of long-term consumption of a translatable typical American diet (TAD) to a comprehensive Mediterranean diet (MD), which is known to have protective properties. This study explored the effect of long0term consumption of the TAD versus the MD on gut microbiome composition. There was an increase of alpha and beta diversity found in the MD compared to the TAD. Additionally, transgenerational effects of these experimental diets found similar results of increased alpha and beta diversity in offspring with perinatal consumption of the MD compared to the TAD. However, these differences were significantly diminished following 2 months of standard diet consumption.